Retrograde adenosine/A_{2A} receptor signaling mediates presynaptic hippocampal LTP and facilitates epileptic seizures

Kaoutsar Nasrallah[1], Coralie Berthoux[1], Yuki Hashimotodani[4], Andrés E. Chávez[5], Michelle Gulfo[1], Rafael Luján[3], Pablo E. Castillo[1, 2, *]

[1] Dominick P. Purpura Department of Neuroscience, [2] Department of Psychiatry & Behavioral Sciences, Albert Einstein College of Medicine, Bronx, NY 10461, U.S.A.; [3] Instituto de Investigación en Discapacidades Neurológicas (IDINE), Facultad de Medicina, Universidad Castilla-La Mancha, 02008 Albacete, Spain.

[4] Present address: Graduate School of Brain Science, Doshisha University, Kyoto, Japan; [5] Present address: Centro Interdisciplinario de Neurociencia de Valparaíso, Facultad de Ciencias, Universidad de Valparaíso, Valparaíso 2340000, Chile

Running title: Adenosine/A_{2A} receptor mediates presynaptic hippocampal LTP

Keywords: Hippocampus, mossy cell, dentate gyrus, retrograde signaling, pattern separation, epilepsy, presynaptic, BDNF, TrkB, PKA.

* To whom correspondence should be addressed:

Pablo E. Castillo, MD/PhD
Dominick P. Purpura Department of Neuroscience
Albert Einstein College of Medicine
1410 Pelham Parkway South
Kennedy Center, Room 703
Bronx, NY 10461, USA
Email: pablo.castillo@einsteinmed.org

Title: 115 characters (with spaces)
Total number of words: Summary: 150; Introduction: 454; Results: 2,173; Discussion: 1,582
Methods: 2,624
Figures: 8; Supplementary figures: 6

Abstract

A long-term change in neurotransmitter release is a widely expressed mechanism controlling neural circuits in the mammalian brain. This presynaptic plasticity is commonly mediated by retrograde signaling whereby a messenger released from the postsynaptic neuron upon activity modifies neurotransmitter release in a long-term manner by targeting a presynaptic receptor. In the dentate gyrus (DG), the main input area of the hippocampus, granule cells (GCs) and mossy cells (MCs) form a recurrent excitatory circuit that is critically involved in DG function and epilepsy. Here, we identified adenosine/A_{2A} receptor ($A_{2A}R$) as a novel retrograde signaling system that mediates presynaptic long-term potentiation (LTP) at MC-GC synapses. Using an adenosine sensor, we found that neuronal activity triggered phasic, postsynaptic TrkB-dependent release of adenosine. Additionally, epileptic seizures released adenosine *in vivo,* while removing $A_{2A}Rs$ from DG decreased seizure susceptibility. Thus, adenosine/$A_{2A}R$ retrograde signaling mediates presynaptic LTP that may contribute to DG-dependent learning and promote epilepsy.

INTRODUCTION

The dentate gyrus (DG), a major input area of the hippocampus, contains two types of excitatory neurons: dentate granule cells (GCs) and hilar mossy cells (MCs). MCs and GCs form an important but under-investigated associative circuit, that is proposed to play a key role in DG-dependent cognitive functions[1,2] and epilepsy[3-5]. Repetitive stimulation of MC axons with physiologically relevant patterns of activity triggers robust presynaptic long-term potentiation at MC-GC synapses (MC-GC LTP)[6]. Remarkably, recent evidence supports that MC-GC LTP can be induced *in vivo* by enriched environment exposure[7], and following experimental epileptic activity[8]. Uncontrolled strengthening of MC-GC transmission promotes seizures and contribute to the pro-epileptic role of MCs in early epilepsy[8]. MC-GC LTP is mechanistically unique. Its induction is NMDA receptor-independent but requires postsynaptic BDNF/TrkB and presynaptic cAMP/PKA signaling[6], strongly suggesting the involvement of a retrograde signal whose identity remains unknown.

Retrograde signaling from the postsynapse to the presynapse is a well-established mechanism implicated in presynaptic forms of long-term plasticity[9]. In this way, the target neuron can strengthen or weaken the synaptic inputs it receives. Diverse messengers have been identified, including lipids, gases, peptides and conventional neurotransmitters[10]. Typically, these messengers are released upon neuronal activity and target a presynaptic receptor (or other molecular target), thereby establishing a retrograde signaling system. The following criteria must be satisfied to establish retrograde signaling as a mechanism of presynaptic long-term plasticity. The retrograde messenger must be synthesized and released from the postsynaptic compartment; interfering with the synthesis and/or release of this messenger should prevent plasticity; the target for the retrograde messenger must be present in the presynaptic bouton; interfering with the presynaptic target should also prevent plasticity; and lastly, activation of the presynaptic target by the retrograde messenger or some analogous molecule should mimic long-term plasticity –although in some cases this activation alone may not be sufficient to mimic plasticity.

In this study, we sought to determine the retrograde signal involved in presynaptic LTP at MC-GC synapses. To our surprise, we found that most conventional retrograde messengers were not implicated in this form of plasticity. Using single-cell manipulations and selective pharmacology, we discovered that activation of G_s-coupled adenosine A_{2A} receptors (A_{2A}Rs) are necessary and sufficient to induce MC-GC LTP. Interfering with adenosine release from a single GC abolished LTP, and immunoelectron microscopy revealed A_{2A}Rs at MC axon terminals. In addition, using a genetically encoded adenosine sensor, we found that neuronal activity triggered phasic release of adenosine in a postsynaptic TrkB-dependent manner. Furthermore, acutely induced epileptic seizures released adenosine *in vivo,* while removing A_{2A}Rs from DG decreased seizure susceptibility. Our findings not only establish adenosine/A_{2A}R as a novel retrograde signaling system that mediates presynaptic plasticity but may also provide a mechanism by which BDNF/TrkB and A_{2A}Rs may promote epileptic activity.

RESULTS

Theta burst firing of a single GC induces presynaptic LTP at MC-GC synapse

To investigate the identity of the retrograde signal mediating MC-GC LTP, we first tested whether activation of a single GC, a manipulation previously used to characterize endocannabinoid retrograde signaling in long-term plasticity[11], could trigger MC-GC LTP. We found that GC theta-burst firing (TBF: 10 bursts at 5 Hz of 5 AP at 50 Hz, repeated 4 times every 5s, **Fig. 1a**) induced LTP selectively at MC-GC synapses but not at neighboring medial perforant path (MPP) inputs (**Fig. 1b**). In addition, the group II mGluR agonist DCG-IV (1 µM), which selectively abolishes GC-MC but not MC-GC transmission[12], did not affect the magnitude of TBF-induced LTP (**Fig. 1f** and **Fig. S1a**), indicating this plasticity does not rely on the recruitment of MCs. Like synaptically-induced MC-GC LTP[6,7], TBF-LTP is likely expressed presynaptically, as indicated by a significant reduction in both paired-pulse ratio (PPR) and coefficient of variation (CV) (**Fig. 1c**). Like synaptically-induced MC-GC LTP, TBF-LTP requires postsynaptic BDNF release, postsynaptic but not presynaptic TrkB, and presynaptic cAMP/PKA signaling. Indeed, TBF-LTP was abolished in the presence of the selective TrkB antagonist ANA-12 (15 µM) (**Fig. S1b** and **Fig. 1f**), and in postsynaptic but not presynaptic *TrkB* conditional knockout (cKO) mice (**Fig. 1d**,**f** and **Fig. S1c**). TBF-LTP was also abolished in postsynaptic *Bdnf* cKO mice, and in GC patch-loaded with botulinum toxin-B (Botox, 0.5 µM; **Fig. S1d,e** and **Fig. 1f**), which blocks BDNF release[13]. The PKA inhibitors, H89 (10 µM, 40- to 60-min pre-incubation and bath applied) (**Fig. S1f** and **Fig. 1f**) and $PKI_{14–22}$ myristoylated (1 µM, 40- to 60-min pre-incubation and bath applied) also abolished TBF-LTP, whereas loading the membrane-impermeant PKI_{6-22} (2.5 µM) in GCs had no effect on this LTP (**Fig. 1e,f**). TBF-LTP was also NMDAR-independent as it was normally induced in the presence of D-APV (50 µM) (**Fig. S1g** and **Fig. 1f**). Lastly, synaptically-induced MC-GC LTP —i.e. burst stimulation (BS) of MC axons— and TBF-LTP occluded each other (**Fig. S2**), strongly suggesting a common mechanism. Thus, the fact that a single-cell manipulation (GC TBF) induced presynaptic LTP of MC-GC transmission with identical properties as synaptically-induced MC-GC LTP, not only strengthens the involvement of retrograde signaling in this form of plasticity, but also establishes a simple tool to investigate the identity of the retrograde messenger as this induction method presumably does not recruit molecular signals arising from neighboring cells.

A non-conventional retrograde signal likely mediates presynaptic LTP at MC-GC synapses

Previous work indicates that retrograde signaling mediating MC-GC LTP does not involve endocannabinoids, glutamate or GABA[6,14], and our current finding that TBF-LTP was normally induced in presynaptic *TrkB* cKO (**Fig. S1c** and **Fig. 1f**), discards BDNF as retrograde messenger. Thus, we tested the role of other conventional retrograde messengers, such as nitric oxide (NO) and lipid-derived messengers [10]. Application of the NO synthase inhibitor L-NAME (100 µM, 50- to 90-min pre-incubation and bath applied)

did not impair TBF-LTP (**Fig. 2a**), but it significantly reduced LTP at CA3-CA1 synapses (**Fig. 2b**), as previously reported[15]. Blockade of lipid-derived messengers with a cocktail of inhibitors consisting of the FAAH and anandamide amidase inhibitor AACOCF3 (10 µM, 50- to 80-min pre-incubation and bath applied), the lipoxygenases inhibitor baicalein (3 µM, 50- to 80-min pre-incubation and bath applied) and the lipase inhibitor THL (tetrahydrolipstatin or orlistat, 4 µM in the recording pipette) did not impair TBF-LTP either (**Fig. 2c**). As positive control, we found that both AACOCF3 and baicalein significantly reduced LTD at CA3-CA1 synapses (**Fig. 2d**) and loading the lipase inhibitor THL (4 µM) in the recording pipette efficiently blocked CA1 inhibitory LTD (iLTD) (**Fig. 2e**)[16]. Lastly, as for TBF-LTP, blocking NO signaling and lipid-derived messengers did not alter synaptically-induced LTP either (**Fig. S3**). Altogether, our results strongly suggest the involvement of a non-conventional retrograde messenger in presynaptic MC-GC LTP.

Presynaptic A_{2A}Rs are required for activity-dependent strengthening of MC-GC synapses

Presynaptic PKA signaling is necessary and sufficient to induce LTP of MC-GC synaptic transmission[6], raising the possibility that the retrograde messenger induces LTP by activating Gs-coupled GPCRs located on MC axon terminals. The Gs-coupled adenosine A_{2A} receptor (A_{2A}R) is a good candidate as it has been implicated in BDNF-mediated plasticity at other synapses[17-19], and the endogenous ligand adenosine can be released from neurons upon activity[20-24]. To test whether adenosine mediates MC-GC LTP by activating presynaptic A_{2A}Rs, we first examined whether LTP induction requires A_{2A}Rs. Remarkably, two different A_{2A}R selective antagonists, SCH 58261 (100 nM) and ZM241385 (50 nM), abolished TBF-LTP (**Fig. 3a**). Moreover, bath application of SCH 58261 did not change basal transmission (**Fig. 3b**) but prevented the induction of LTP by BDNF puffs (8 nM, 2 puffs of 3 s) delivered in the inner molecular layer (IML) (**Fig. 3c**)[6], suggesting that A_{2A}R activation is required downstream of the BDNF/TrkB cascade. Postsynaptic A_{2A}Rs were not involved given that including the G-coupled protein inhibitor GDPβs (1 mM) in the recording pipette did not affect TBF-LTP, (**Fig. 3d**), whereas it abolished the change in holding current induced by the selective $GABA_B$ receptor agonist baclofen (10 µM) (**Fig. 3d**). Likewise, BS-induced LTP was also abolished by SCH 58261 (**Fig. S4a**), but not by including GDPβs in the recording pipette (**Fig. S4b**). To demonstrate the role of presynaptic A_{2A}Rs in MC-GC LTP, we also employed a conditional knockout strategy combined with optogenetics which allow us to selectively activate A_{2A}R-deficient MC axons expressing the fast opsin ChIEF (**Fig. 3e**). We found that presynaptic A_{2A}R cKO abolished TBF-LTP (**Fig. 3f**). Taken together, these findings indicate that presynaptic but not postsynaptic A_{2A}R activation was necessary for LTP at MC-GC synapses.

A_{2A}Rs are likely activated by adenosine released from GCs during LTP induction. As adenosine can also target presynaptic adenosine type 1 receptors (A_1Rs), $G_{i/o}$-coupled receptors whose activation typically suppress neurotransmitter release, we therefore tested the role of A_1Rs in this LTP. Indeed, the selective A_1R antagonist DPCPX (100 nM) significantly increased MC-GC LTP magnitude (**Fig. 3g**), whereas it had no effect on basal transmission (**Fig. 3h**), indicating that A_1Rs negatively control MC-GC LTP.

Activation of presynaptic A_{2A}Rs induces MC-GC LTP in a PKA-dependent manner

Our results strongly suggest that MC terminals express functional A_1Rs and A_{2A}Rs (**Fig. 3**). To directly assess this possibility, we performed immunoelectron microscopy. Immunoparticles for A_1Rs were mainly found presynaptically in the molecular layer of the dentate gyrus at MC-GC and perforant path (PP)-GC synapses (**Fig. 4a-d**). Remarkably, using an anti-A_{2A}R antibody previously validated in in A_{2A}R-deficient mice[25], we found strong A_{2A}R expression in the presynaptic membrane of asymmetric, putative MC-GC synapses in the IML (**Fig. 4e,f,h**) and very few particles postsynaptically (**Fig. 4e,f,h**). In contrast, a quasi-exclusive postsynaptic expression was detected at asymmetric PP-GC synapses (**Fig. 4g-h**).

We next tested whether A_{2A}R activation was sufficient to induce LTP at MC-GC synapses. Bath application of the A_{2A}R agonist CGS21680 (50 nM, 15 min) selectively enhanced MC but not MPP EPSC amplitude (**Fig. 5a**). This synapse-specific potentiation was associated with a significant decrease in both PPR and CV (**Fig. 5b**), suggesting a presynaptic mechanism of expression, and supporting a presynaptic location of A_{2A}Rs. Adding the selective A_{2A}R antagonist SCH 58261 (100 nM) during the washout of CGS21680 (50 nM) did not impair the long-lasting potentiation, whereas continuous bath application of SCH 58261 (100 nM) abolished the CGS21680-induced potentiation (**Fig. 5c**). These results indicate that activation of A_{2A}Rs was sufficient to induce LTP at MC-GC synapses. Because the A_{2A}R is a Gs-coupled receptor, we next tested whether CGS21680-induced LTP was PKA-dependent. Bath application of the selective, cell-permeant PKA inhibitor myristoylated PKI_{14-22} (1 µM) abolished CGS21680-induced LTP, whereas loading the membrane-impermeant PKA inhibitor PKI_{6-22} (2.5 µM) in GCs via the recording pipette had no effect (**Fig. 5d**). Thus, A_{2A}Rs enhance glutamate release via presynaptic PKA activation, consistent with previous findings showing that PKA activity is necessary and sufficient for MC-GC LTP[6].

Our results thus far indicate that both BDNF/TrkB and adenosine/A_{2A}R signaling are involved in MC-GC LTP, and previous work demonstrated that A_{2A}Rs facilitate BDNF signaling at some synapses[17]. We therefore sought to determine potential interactions between these signaling cascades at the MC-GC synapse. The TrkB antagonist ANA-12 had no effect on CGS21680-induced LTP (**Fig. 5e**), whereas it blocked TBF-LTP in interleaved experiments (**Fig. 5f**; see also **Fig. S1b**). These findings, together with our previous results (**Fig. 3, 4**), strongly suggest that presynaptic adenosine/A_{2A}R signaling mediates LTP downstream of BDNF/TrkB signaling.

MC axon terminals also express A_1Rs (**Fig. 4**) whose activation could trigger presynaptic long-term depression[26]. However, bath application of the selective A_1R agonist CCPA (50 nM, 15 min) reduced both MC and MPP-mediated transmission reversibly as the reduction was washed out with the A_1R antagonist DPCPX (100 nM) (**Fig. S5a**). This transient A_1R-induced depression was associated with a reversible increase in both PPR and CV (**Fig. S5b,c**), suggesting a presynaptic mechanism. CCPA (50 nM, 15 min) failed to induce synaptic depression in the presence of DPCPX (100 nM) (**Fig. S5,d**). Thus, although both

A_1 and A_{2A} receptors are expressed at MC axon terminals, only the latter engages long-lasting synaptic plasticity.

Passive adenosine release from GC is required for presynaptic MC-GC LTP

Adenosine can be released from neurons upon activity[20,22-24] via equilibrative nucleoside transporters (ENTs)[21]. Our results strongly suggest that presynaptic A_{2A}Rs are activated by endogenous adenosine during MC-GC LTP (**Fig. 3**). If adenosine is the retrograde signal, interfering with adenosine release selectively from GCs should impair LTP. As a first approach, we tested whether blocking ENTs can interfere with LTP induction. Bath application of the ENTs inhibitors dipyridamole (20 μM) and NBMPR (10 μM) abolished LTP (**Fig. 6a**) but did not affect basal MC-GC synaptic transmission (**Fig. 6b**). Because ENTs are also implicated in adenosine reuptake, bath application of the ENT blockers may significantly increase extracellular adenosine levels, which, by activating A_{2A}Rs may potentiate MC-GC transmission and occlude LTP. The fact that ENT blockers had no effect on basal MC-GC synaptic transmission (**Fig. 6b**) could be due to simultaneous activation of A_1R, which might mask any potential A_{2A}R-mediated potentiation. To test this possibility, we bath applied both the ENT blockers and DPCPX (100 nM) to prevent a potential A_1R-mediated depression of MC-GC synaptic transmission. We found that co-application of the ENT blockers and DPCPX (100 nM) increased MC-GC transmission, and this effect was abolished in the presence of the A_{2A}R antagonist SCH 58261 (100 nM) (**Fig. 6c**). These results indicate that increasing the extracellular concentration of endogenous adenosine is sufficient to activate presynaptic A_{2A}R and trigger MC-GC potentiation.

To avoid adenosine tonic activity due to extracellular accumulation, we employed a single-cell approach and selectively blocked ENTs in a single GC. Similarly to previous studies[22,24], we loaded inosine (100 μM) intracellularly, a competitive blocker of adenosine efflux through ENTs[21], *via* the recording pipette. We found that intracellular inosine abolished TBF-LTP (**Fig. 6d**), whereas bath application of 100 μM inosine had no effect on MC-GC synaptic transmission (**Fig. 6e**). Bath application of DPCPX increased MC EPSC amplitude when ENTs inhibitors were continuously bath applied but not when inosine (100 μM) was loaded in a single GC (**Fig. 6f**), confirming that intracellular inosine did not increase adenosine tone. Altogether these findings indicate that adenosine, passively released from GC through ENTs, likely acts as a retrograde messenger at MC-GC synapses.

Repetitive neuronal activity induces adenosine release via a BDNF/TrkB-dependent mechanism

To test whether adenosine is released during MC-GC LTP induction, we utilized the genetically encoded sensor for adenosine $GRAB_{Ado1.0m}$[27] selectively expressed in commissural MC axons (see Methods), and found a clear fluorescence signal in the contralateral IML (Fig. **7a,b**). The MC BS protocol that triggers MC-GC LTP in acute hippocampal slices also induced a transient increase in the $GRAB_{Ado1.0m}$ signal. As expected[27], this enhancement was abolished when the MC BS protocol was delivered in

the presence of the $A_{2A}R$ antagonist SCH58261 (**Fig. 7b,c,f**). Consistent with $A_{2A}R$ signaling being engaged downstream of TrkB activation, we found no change in $GRAB_{Ado1.0m}$ fluorescence in the presence of the TrkB antagonist ANA-12 (15 μM), and in postsynaptic *TrkB* cKO mice (**Fig. 7d,e,f**). Altogether these results demonstrate that MC repetitive activity releases adenosine in a postsynaptic TrkB-dependent manner.

Lastly, we aimed to determine whether neuronal activity induces adenosine release *in vivo* and the functional impact of such release. We recently found that MC-GC LTP can also be triggered by early epileptic activity induced with kainic acid (KA) intraperitoneal (i.p.) administration, and this LTP further promotes seizure activity[8]. Therefore, we hypothesized that epileptic activity should release adenosine, and interfering with adenosine/$A_{2A}R$ signaling should reduce seizures. To test these predictions, we expressed $GRAB_{Ado1.0m}$ in commissural MC axons and recorded the fluorescence signals using fiber photometry in freely moving mice (**Fig. 8a,b**). We found a large increase in $GRAB_{Ado1.0m}$ fluorescence following i.p. injection of KA (**Fig. 8c,d**) but not saline (not shown). Moreover, $A_{2A}R$ deletion from DG excitatory neurons, which blocked MC-GC LTP *in vitro* (**Fig. 3**), reduced KA-induced seizure susceptibility and severity (**Fig. 8e-i**). Altogether, these results not only demonstrate *in vivo* adenosine release following neuronal activity that occur during initial seizures, but strongly suggest that adenosine signaling promotes seizures via $A_{2A}Rs$.

DISCUSSION (1,558 words)

In this study, we discovered a novel retrograde signaling mechanism that mediates presynaptic activity-dependent synaptic strengthening, at an important but long-overlooked hippocampal circuit (**Fig. S6**). Specifically, we found that repetitive firing of a single postsynaptic neuron was sufficient to trigger presynaptic LTP at MC-GC but not neighboring MPP synapses. We demonstrated that functional A_{2A} receptors are expressed at MC axon terminals but not at MPP axon terminals, and that $A_{2A}R$ activation is necessary and sufficient to induce MC-GC LTP. During LTP induction GCs passively release adenosine through ENTs, in a postsynaptic TrkB- and activity-dependent manner. Moreover, we found that adenosine is released *in vivo* during initial seizures and $A_{2A}R$ cKO has an anti-epileptic effect. Our findings establish adenosine/$A_{2A}R$ as a novel retrograde signaling mechanism not only relevant to synaptic plasticity but also to early epileptogenesis.

GC TBF induces presynaptic LTP at MC-GC synapses

We previously showed that MC bursts of activity powerfully induce MC-GC LTP[6]. The present study revealed that direct activation of a single GC with physiologically relevant pattern of activity[28-33] was sufficient to induce presynaptic LTP at MC-GC synapses without changing the strength of MPP neighboring inputs. Against the possibility that this single cell-induced LTP could emerge from the activation of the recurrent GC-MC-GC circuit are the following two observations. First, GC TBF induced normal LTP even in

continuous presence of the selective group II mGluR agonist DCG IV, which abolishes GC-MC[34,35] but not MC-GC transmission[12]. Second, TBF LTP was normally induced at optogenetically activated synaptic inputs arising from contralateral MC axons that are separated from their cell bodies in hippocampal slices. Importantly, our results strongly suggest that GC TBF and synaptically (MC BS)-induced LTP share a common mechanism that involves postsynaptic BDNF/TrkB and presynaptic adenosine/A_{2A}R and cAMP/PKA signaling. In addition, both potentiations are expressed presynaptically. We recently found that synaptically-induced MC-GC LTP requires BDNF release from GCs[7]. It is therefore likely that GC TBF induces LTP in part by releasing BDNF from the postsynaptic compartment. Consistent with this possibility, we now report that GC TBF-induced LTP requires both dendritic BDNF release via SNARE-dependent exocytosis as also reported in cortical neurons and hippocampal slices[13,36].

Adenosine is released from GC in an activity and TrkB-dependent manner

Using the genetically encoded adenosine sensor $GRAB_{Ado1.0m}$[27], we detected a phasic increase in extracellular adenosine following both LTP induction *ex vivo* and during epileptic activity *in vivo*. Previous studies have shown that adenosine can be released from neurons upon activity via ENTs[20-24]. In support of this mechanism, we found that interfering with ENT-mediated release of adenosine from a single postsynaptic GC abolished MC-GC LTP, indicating that passive release of adenosine from GCs is crucial for this form of plasticity. However, we cannot discard a potential contribution of adenosine arising from ATP extracellular conversion[37,38] or from other cell types such as interneurons and glial cells[20,39].

Intracellular accumulation of adenosine can be the consequence of sequential dephosphorylation of ATP or the hydrolysis of S-adenosylho-mocysteine[40]. During MC-GC LTP induction, formation of intracellular adenosine in GCs likely results from robust postsynaptic TrkB activation, which presumably causes sequential dephosphorylation of ATP. In support of this scenario are the following observations. First, MC-GC LTP induction releases BDNF that activates TrkB receptors on GCs[6,7]. Second, activity-induced adenosine release in the IML is postsynaptic TrkB-dependent, as it is abolished in the presence of the TrkB selective antagonist ANA-12 and by genetically removing *TrkB* from GCs. Third, adenosine/A_{2A}R signaling is engaged downstream of TrkB activation, as indicated by the fact that BDNF-induced LTP was abolished by A_{2A}R antagonism, whereas TrkB antagonism had no effect on A_{2A}R agonist-induced LTP. Lastly, adenosine acts via presynaptic A_{2A}Rs, whereas BDNF activates postsynaptic TrkB[6,7], discarding physical interaction or transactivation, a process whereby A_{2A}R activation can induce TrkB phosphorylation in the absence of neurotrophins[41].

To our knowledge, we provide the first direct evidence that adenosine release can occur in a TrkB-dependent manner. Such a mechanism could explain, at least in part, BDNF and adenosine signaling interactions reported at other synapses in the brain. Several studies showed that activation of the G_s-coupled A_{2A}R and PKA are required for BDNF-induced facilitation of synaptic transmission and plasticity. Although such observations

have been extensively reported in the hippocampus[17-19,42,43], the precise mechanism of this crosstalk remains elusive. Consistent with our findings at the hippocampal MC-GC synapse, BDNF-induced facilitation at the neuromuscular junction was abolished in presence of $A_{2A}R$ antagonists but also by PKA inhibitors, while $A_{2A}R$ agonist-induced increase in neurotransmitter release is TrkB-independent[17,42,43]. In conclusion, our findings support a model whereby neuronal activity releases adenosine in TrkB-dependent manner. Further work is required to determine the generalizability of this model in other brain areas and to identify the precise mechanisms whereby TrkB activation leads to adenosine release.

Retrograde adenosine/$A_{2A}R$ cascade mediates presynaptic LTP at MC-GC synapses

Retrograde signaling is a common mechanism in presynaptic forms of long-term plasticity[9]. While several retrograde signals have been identified throughout the brain[10]; here we uncovered adenosine/$A_{2A}R$ as a novel form of retrograde signaling in the hippocampus. Single cell manipulations revealed that interfering with adenosine release from a single postsynaptic neuron completely abolished MC-GC LTP, induced by GC firing alone. Furthermore, by using pharmacology, $A_{2A}R$ presynaptic cKO and electron microscopy, we demonstrated that activation of presynaptic $A_{2A}Rs$ was necessary and sufficient for MC-GC LTP. However, we cannot discard potential role of other cell-types, including glial cells, as potential source or target of adenosine. Despite the relatively low expression levels of $A_{2A}R$ in the hippocampus[44], previous work has demonstrated that $A_{2A}R$ signaling can regulate hippocampal synaptic plasticity[45,46]. To our knowledge, our study provides the first evidence that retrograde adenosine signaling can mediate presynaptic LTP. As Gs-coupled receptors, $A_{2A}Rs$ on MC axon terminals likely activate the cAMP/PKA cascade, and as for other forms of presynaptic LTP[9], this activation engages a long-lasting increase of glutamate release whose downstream mechanism is poorly understood. Whether retrograde adenosine/$A_{2A}R$ signaling can mediate activity-dependent strengthening at other synapses in the brain remain to be investigated.

Role of A_1Rs in controlling MC-GC synaptic transmission and LTP

As previously reported at other synapses[42,47], our findings strongly suggest that endogenous adenosine simultaneously activate A_1R and $A_{2A}R$ localized at MC terminals. While there is evidence that A_1R and $A_{2A}R$ can localize at the same nerve terminal[48] and even form heteromers[49], our results cannot deny or support these possibilities. The induction of MC-GC LTP was associated with a surge of extracellular adenosine that triggered LTP via $A_{2A}R$ activation, but dampened LTP via A_1R activation. While A_1R agonism transiently inhibited glutamate release, $A_{2A}R$ agonism increased glutamate release in a long-lasting manner. Consistent with these pharmacological observations, the net effect mediated by transient release of endogenous adenosine during LTP induction was a long-lasting enhancement of glutamate release. Similar A_1R-mediated dampening of LTP has previously been observed at other synapses[50,51]. A possible explanation for this dampening is that presynaptic A_1Rs, which are $G_{i/o}$-coupled, decrease the level of

cAMP required for MC-GC LTP[6]. We recently reported that the type 1 cannabinoid receptor, another $G_{i/o}$-coupled receptor that is highly expressed at MC axon terminals, also dampens MC-GC LTP[14]. Thus, the induction of this form of plasticity is tightly controlled by two distinct retrograde signals, adenosine and endocannabinoids, which by activating presynaptic $G_{i/o}$-coupled receptors dampen LTP induction. In this way, both retrograde signals could prevent runaway activity of the MC-GC-MC recurrent excitatory circuit. Notably, we did not find any tonic regulation of basal transmission by A_1R nor $A_{2A}R$ at MC-GC synapse.

Physiological and pathological relevance of $A_{2A}R$-mediated LTP in the dentate gyrus

Growing evidence indicates that MCs are critically involved in hippocampal-dependent learning[2]. For example, silencing MCs, selectively, impairs retrieval of spatial memory[52] and novelty-induced contextual memory acquisition[53]. MC-GC LTP is a robust form of presynaptic plasticity that can be elicited in vivo upon experience[7] and, by changing information flow in the DG[6], it may contribute significantly to learning and memory. While GCs exhibit extremely sparse and selective firing in single place field[30], we found that MC-GC LTP can be triggered by GC firing alone, suggesting that this plasticity could be implicated in experience-driven refinement of DG circuit and memory. Previous work indicates that adenosine/$A_{2A}R$ signaling may contribute to hippocampal-dependent memory[46,49]. Our findings demonstrating a key role for adenosine/$A_{2A}R$ signaling in MC-GC LTP could explain, at least in part, memory impairments found in both $A_{2A}R$ antagonist-injected animals[54] and hippocampal $A_{2A}R$ cKO[55]. Demonstrating the precise role of adenosine$A_{2A}R$ retrograde signaling at MC-GC synapses will necessitate selective manipulation of $A_{2A}Rs$ at MC axon terminals, a task requiring tools that are not currently available.

Adenosinergic signaling is critically involved in epilepsy[56]. Global $A_{2A}R$ genetic deletion and selective $A_{2A}R$ antagonism attenuates both seizures progression[57,58] and seizures-induced neuronal damage[59-61], whereas $A_{2A}R$ activation lowers seizures' threshold[62]. In addition, decreased A_1R signaling and increased A_{2A}[63] and BDNF/TrkB signaling[64] occurs in epilepsy. Remarkably, we found that MC-GC LTP required TrkB-dependent adenosine/$A_{2A}R$ signaling while its induction was negatively regulated by adenosine A_1R activity. Although the precise mechanism by which $A_{2A}Rs$ participate in temporal lobe epilepsy is poorly understood, presynaptic $A_{2A}Rs$ at MC axons may explain, at least in part, the pro-epileptic role of $A_{2A}Rs$ and the antiepileptic role of A_1Rs. This notion is consistent with our recent work demonstrating that initial seizures trigger MC-GC LTP broadly in the DG and that uncontrolled LTP is sufficient to promote subsequent seizures[8]. Our new study demonstrating adenosine/$A_{2A}R$-dependent strengthening of MC-GC synapses provides not only a novel mechanism whereby MC activity may contribute to early stages of temporal lobe epilepsy [2,5,8,65], but also highlights a potential target for the treatment of this disorder.

METHODS

Experimental Model and Subject Details

Sprague-Dawley rats P19-P30 and P50-P70 C57BL/6, floxed TrkB (*TrkB*$^{fl/fl}$), floxed BDNF (*Bdnf*$^{fl/fl}$) and floxed $A_{2A}R$ (*A*$_{2A}$*R*$^{fl/fl}$) mice were used. Males and females were equally used. All animals were group housed in a standard 12 hr light/12 hr dark cycle and had free access to food and water. Animal handling and use followed a protocol approved by the Institutional Animal Care and Use Committee of Albert Einstein College of Medicine, in accordance with the National Institutes of Health guidelines. *TrkB*$^{fl/fl}$ and *Bdnf*$^{fl/fl}$ mice generated by Dr. Luis Parada, were kindly donated by Dr. Lisa Monteggia (University of Texas, Southwestern Medical Center). *Adora2*$^{fl/fl}$ were obtained from Jackson Laboratory (B6;129-Adora2atm1Dyj/J, Jax 010687).

Hippocampal slice preparation

Acute transverse hippocampal slices were prepared from Sprague-Dawley rats (400 µm thick) and mice (300-µm thick). Animals were anesthetized with isofluorane and euthanized in accordance with institutional regulations. The hippocampi were then removed and cut using a VT1200s microslicer (Leica Microsystems Co.) in a cutting solution. Hippocampal slices from rats were prepared using a cutting solution containing (in mM): 215 sucrose, 2.5 KCl, 26 $NaHCO_3$, 1.6 NaH_2PO_4, 1 $CaCl_2$, 4 $MgCl_2$, 4 $MgSO_4$ and 20 D-glucose. 30 min post-sectioning, the cutting medium was gradually switched to extracellular artificial cerebrospinal (ACSF) recording solution containing (in mM): 124 NaCl, 2.5 KCl, 26 $NaHCO_3$, 1 NaH_2PO_4, 2.5 $CaCl_2$, 1.3 $MgSO_4$ and 10 D-glucose. Slices were incubated for at least 40 min in the ACSF solution before recording. Mouse hippocampal slices were prepared using a NMDG-based cutting solution containing (in mM): 93 N-Methyl-d-glucamin, 2.5 KCl, 1.25 NaH_2PO_4, 30 $NaHCO_3$, 20 HEPES, 25 D-glucose, 2 Thiourea, 5 Na-Ascorbate, 3 Na-Pyruvate, 0.5 $CaCl_2$, 10 $MgCl_2$. These slices were then transferred to 32°C ACSF for 30 min and then kept at room temperature for at least 1h before recording. All solutions were equilibrated with 95% O_2 and 5% CO_2 (pH 7.4).

Electrophysiology

Recordings were performed at 28 ± 1°C, otherwise stated, in a submersion-type recording chamber perfused at 2 mL/min with ACSF supplemented with the $GABA_A$ and the $GABA_B$ receptor antagonists, picrotoxin (100 µM) and CGP55845 hydrochloride (3 µM). Whole-cell patch-clamp recordings using a Multiclamp 700A amplifier (Molecular Devices) were obtained from GCs voltage clamped at −60 mV using patch-type pipette electrodes (~3-4 MΩ) containing (in mM): 135 $KMeSO_4$, 5 KCl, 1 $CaCl_2$, 5 NaOH, 10 HEPES, 5 MgATP, 0.4 Na_3GTP, 5 EGTA and 10 D-glucose, pH 7.2 (288-291 mOsm). For IPSC recording in CA1, whole cell voltage clamp recordings were obtained from CA1 pyramidal neurons voltage clamped at V_h= 10 mV using a cesium-based internal solution containing (in mM): 131 cesium gluconate, 8 NaCl, 1 $CaCl_2$, 10 EGTA, 10 D-glucose and 10 HEPES, pH 7.2 (285-290 mOsm). IPSCs were evoked using an electrical stimulating pipette placed in CA1 *stratum radiatum*, and recordings were performed in the continuous presence of ionotropic glutamate receptor antagonists NBQX (10 µM) and D-APV (50 µM). LTD of inhibitory

inputs onto CA1 pyramidal neurons (iLTD) was induced using theta burst-stimulation protocol (TBS, 10 bursts at 5 Hz of 5 pulses at 100 Hz, repeated every 5 s, 4 times). Series resistance (~6-25 MΩ) was monitored throughout all experiments with a −5 mV, 80 ms voltage step, and cells that exhibited a significant change in series resistance (> 15%) were excluded from analysis. Botox experiments were performed at 32 °C. Botox was supplemented with 5 mM dithiothreitol (DTT) in the intracellular solution, and interleaved control experiments included DTT only.

A broken tip (~10–20 µm) stimulating patch-type micropipette filled with ACSF was placed in the inner molecular layer (IML, < 50 µm from the border of the GC body layer) to activate MC axons, and in the middle third of the molecular layer to activate MPP inputs. To elicit synaptic responses, paired, monopolar square-wave voltage or current pulses (100–200 µs pulse width, 4-27 V) were delivered through a stimulus isolator (Digitimer DS2A-MKII). Typically, stimulation intensity was adjusted to obtain synaptic responses comparable in amplitude across experiments; e.g., 30-70 pA EPSCs (V_h −60 mV). For the optogenetic experiments, EPSCs were evoked using 1-3 ms pulses of blue (470-nm) light, provided by a collimated LED (Thorlabs, M470L3-C5, 470 nm, 300mW) and delivered through the microscope objective (40X, 0.8 NA). GC TBF-induced LTP was typically induced with 10 bursts at 5 Hz of 5 AP at 50 Hz, repeated 4 times every 5s, while the membrane potential was held at −60 mV in current clamp. Extracellular field recordings were performed using patch-type pipettes filled with 1M NaCl, placed in *CA1 stratum radiatum*. fESPS were evoked with an ACSF-containing broken tip patch pipette in *CA1 stratum radiatum*. LTP at CA3-CA1 synapses, was triggered using high frequency stimulation protocol (4 HFS: 100 pulses at 100 Hz repeated 4 times every 10 s) and recordings were performed at 25 ± 1°C. LTD was induced with low frequency stimulation protocol (LFS: 900 pulses at 1 Hz).

Electrophysiological data were acquired at 5 kHz, filtered at 2.4 kHz, and analyzed using custom-made software for IgorPro (Wavemetrics Inc.). Paired-pulse ratio (PPR) was defined as the ratio of the amplitude of the second EPSC (baseline taken 1-2 ms before the stimulus artifact) to the amplitude of the first EPSC. Coeficient of variation (CV) was calculated as the standard deviation of EPSC amplitude divided by mean EPSC amplitude. Both PPR and CV were measured 10 min before and 20–30 min after LTP induction protocol or CGS21680-induced potentiation. The magnitude of LTP/LTD was determined by comparing 10 min baseline responses with responses 20-30 min (or 30-40 min for **Fig. 1b**, 40-50 min for **Fig. 2b**, 45-55 min for **Fig. 2d**) after induction protocol. Averaged traces include 20 consecutive individual responses.

Postsynaptic TrkB and BDNF conditional KO

Adeno-associated virus AAV_5.CamKII.eGFP (control virus) or AAV_5.CamKII.GFP-CRE (University of Pennsylvania Vector Core) was injected (1 µL at a flow rate of 0.1 µL/min) unilaterally into the dorsal blade of the dentate gyrus (2.06 mm posterior to bregma, 1.5 mm lateral to bregma, 1.8 mm ventral from dura) of *TrkB*$^{fl/fl}$ or *Bdnf*$^{fl/fl}$ mice (4-5 week old). Animals were placed in a stereotaxic frame and anesthetized with isoflurane (up to 5% for

induction and 1%–3% for maintenance). Both male and female mice were used with a similar ratio for the two types of viruses. Slices for electrophysiology were prepared from injected animals 3–5 weeks after injection. For each animal, the absence of GFP-expressing cells in the hilus of the entire ipsilateral hippocampus was verified.

Presynaptic TrkB and $A_{2A}R$ conditional KO

A mix with (1:2 ratio, 1.2 µL at 0.1 µL/min) of Cre recombinase-containing AAV (AAV_5.CamKII.Cre-mCherry, UNC Vector) and Cre-dependent ChiEF (AAV_{DJ}.Flx.ChIEF.Tdtomato) was injected into the dentate gyrus (relative to bregma: 1.9 mm posterior, 1.25 mm lateral, 2.3 ventral) of adult *TrkB*$^{fl/fl}$, *A*$_{2A}$*R*$^{fl/fl}$ or WT control mice (4-5 week old). We then performed electrophysiology experiments 4–5 weeks post-injection in contralateral hippocampal slices. This allowed us to optically activate Cre-expressing MC axons.

Pharmacology

Reagents were bath applied following dilution into ACSF from stock solutions stored at −20°C prepared in water, DMSO or ethanol, depending on the manufacturer's recommendation. BDNF puffs (8 nM, 2.5-3 PSI, 3 s puffs repeated twice, 5 s interval) were applied using a Picospritzer III (Parker) connected to a broken patch pipette. The tip of the puffer pipette was positioned above the IML while monitoring MC-GC transmission. For experiments requiring postsynaptic loading PKI_{6-22}, LTP was induced at least 20 min after establishing the whole-cell configuration. Time of LTP induction protocol was matched in interleaved controls.

Electron Microscopy

Animal care and handling prior to and during the experimental procedures were in accordance with Spanish (RD 1201/2005) and European Union (86/609/EC) regulations, and the protocols were approved by the University's Animal Care and Use Committee. Mice were anesthetized by intraperitoneal injection of ketamine⁄xylazine (ratio 1:1, 0.1 mL/kg) and transcardially perfused with ice-cold fixative containing 4% paraformaldehyde, with 0.05% glutaraldehyde and 15% (v/v) saturated picric acid made up in 0.1 M phosphate buffer (PB, pH 7.4). Brains were then removed and immersed in the same fixative for 2 hours or overnight at 4°C. Tissue blocks were washed thoroughly in 0.1 M PB. Coronal sections (60-µm thick) were cut using a vibratome (Leica V1000). Pre-embedding immunohistochemical analyses was performed as described previously[66]. Free-floating sections were incubated in 10% (v/v) NGS diluted in TBS. Sections were then incubated in, 3-5 µg/mL diluted in TBS containing 1% (v/v) NGS, anti-$A_{2A}R$ [guinea pig anti-$A_{2A}R$ polyclonal (AB_2571656; Frontier Institute co., Japan)] or anti-A_1R [rabbit-anti-A_1R antibody (2 mg/ml; Affinity Bioreagents, Labome, USA] antibodies, followed by incubation in goat anti-guinea pig IgG coupled to 1.4 nm gold or in goat anti-rabbit IgG coupled to 1.4 nm gold (Nanoprobes Inc., Stony Brook, NY, USA), respectively. Sections were postfixed in 1% (v/v) glutaraldehyde and washed in double-distilled water, followed by silver enhancement of the gold particles with an HQ Silver kit (Nanoprobes Inc.). Sections were then treated with osmium tetraoxide (1% in 0.1 m phosphate buffer), block-stained with uranyl acetate, dehydrated in graded series of ethanol and flat-embedded on

glass slides in Durcupan (Fluka) resin. Regions of interest were cut at 70-90 nm on an ultramicrotome (Reichert Ultracut E, Leica, Austria) and collected on single slot pioloform-coated copper grids. Staining was performed on drops of 1% aqueous uranyl acetate followed by Reynolds's lead citrate. Ultrastructural analyses were performed in a Jeol-1010 electron microscope. Quantitative analysis of the relative abundance of $A_{2A}R$ or A_1R, in the molecular layer of the dentate gyrus, was performed from 60 µm coronal slices as described[66], in the area for MC-GC synapses and the area of PP-GC synapses. For each of three animals, three samples of tissue were obtained (nine total blocks). Electron microscopic serial ultrathin sections were cut close to the surface of each block because immunoreactivity decreased with depth. Randomly selected areas were captured at a final magnification of 45,000X, and measurements covered a total section area of ~5000 µm^2. Dendritic shafts, dendritic spines and axon terminals were assessed for the presence of immunoparticles. The percentage of immunoparticles for $A_{2A}Rs$ or for A_1Rs at postsynaptic and presynaptic sites was calculated. To establish the relative frequency of $A_{2A}R$ in axon terminals, immunoparticles identified in this compartment were counted. The perimeter of each axon terminal was measured in reference areas totaling ~2,000 µm^2. All axon terminals establishing excitatory synapses were counted and assessed from single ultrathin sections.

Two-photon live imaging of $GRAB_{Ado}$ in acute hippocampal slices

AAV_9.hSyn.GRAB.Ado1.0m (WZ Biosciences Inc) was injected (1 µL at 0.1 µL/min) unilaterally into the hilus of WT mice or *TrkB$^{fl/fl}$* mice (3 - 4 week old). Slices were prepared 3 - 4 weeks post-injection and expression of $GRAB_{Ado1.0m}$ was confirmed in MCs of the ipsilateral hippocampus for each injected mouse. Hippocampal slices from $GRAB_{Ado1.0m}$-injected mice were prepared using an ice-cold dissection buffer maintained in 5% CO_2/95% O2 and containing (in mM): 25 NaHCO3, 1.25 NaH_2PO_4, 2.5 KCl, 0.5 $CaCl_2$, 7 $MgCl_2$, 25 D-glucose, 110 choline chloride, 11.6 ascorbic acid, 3.1 pyruvic acid. Slices were transferred to 32°C ACSF for 30 min and kept at room temperature for at least 45 min before imaging. Slices were then transferred to an imaging chamber under an Ultima 2-photon microscope (Bruker Corp.) equipped with a 60X NA 1.0 water-immersion objective and InSight DeepSee laser (Spectra-Physics). A 920-nm laser was used to excite $GRAB_{Ado1.0m}$, and the emission signal was acquired using a 525–570 nm band-pass filter. The field of view (512 x 512 pixels per frame) was chosen in the IML of contralateral hippocampal slices where MC commissural axons projected onto GCs and expressed $GRAB_{Ado1.0m}$. A broken tip stimulating patch-type micropipette filled with ACSF was positioned in the IML ~150 µm from the imaging region to activate MC axons. The region of interest (ROI) was magnified to 2X and at least 40 consecutive images (at 0.25 Hz) as a baseline using a PrairieView 5.4 (Bruker Corp.). Following baseline acquisition, MC burst stimulation was applied and at least additional 100 images (at 0.25 Hz). To verify reactivity of the ROI adenosine (100 µM) was added at the end of the imaging session. The fluorescence intensity of the ROI was measured and the $\Delta F/F_0$ of the $GRAB_{Ado1.0m}$ signal was calculated using ImageJ software. All recordings were performed at 28 ± 1°C in a submersion-type recording chamber perfused at 2 mL/min with ACSF.

Seizure induction and monitoring

Epileptic seizures were induced acutely in 2-3–month-old mice. Intraperitoneal (IP) injection of 20-30 mg/kg of kainic acid (KA, HelloBio HB0355) prepared in saline solution the same day were performed. For behavioral seizure scoring, mice were monitored during 120 min post-injection and behavioral seizures were scored, by an experimenter blind to condition (control *vs* $A_{2A}R$ cKO), using a modified Racine scale as follows: stage 0: normal behavior, stage 1: immobility and rigidity, stage 2: head bobbing, stage 3: forelimb clonus and rearing, stage 4: continuous rearing and falling, stage 5: clonic-tonic seizure, stage 6: death. The maximum Racine score was recorded every 10 minutes and the cumulative seizure score was obtained by summing these scores across all 12 bins of the 120 min experiment.

Fiber photometry in freely behaving mice

AAV_9.hSyn.GRAB.Ado1.0m (1.2 µL at 0.1 µL/min) was unilaterally injected into the DG (relative to bregma: 1.9 mm posterior, 1.25 mm lateral, 2.3 ventral) of WT mice (5-6 week old). An optic fiber (200 µm diameter, NA = 0.37, Neurophotometrics) was implanted unilaterally, into the contralateral DG above the IML (relative to bregma: 1.9 mm posterior, 1.25 mm lateral, 1.8 mm ventral) to record $GRAB_{Ado1.0m}$ fluorescence *in vivo*. 3-5 weeks after surgery, the fluorescence signal was monitored before and after KA IP injection (30 mg/kg). To record $GRAB_{Ado1.0m}$ fluorescence, a three-channel multi-fiber photometry system (Neurophotometrics v1 Ltd) was used. 470 nm and 415 nm out of phase excitation lights were bandpass filtered and directed via a 20X objective (power: 30 µW). A single patch cord connected to the optic fiber implant was used to deliver light and collect the emitted fluorescence, which was filtered, and projected on a CMOS camera sensor. The open-source software Bonsai was used for data acquisition (40 frames/s rate). The fluorescence intensity profile of each channel was calculated as the mean pixel value of the region of interest. To calculate $\Delta F/F_0$, the 470 nm-evoked signal was normalized by the isosbestic signal (415 nm) to correct for photobleaching and potential artefacts. F_0 corresponds to the average of the last three-minute (baseline) before KA injection.

Post-hoc analysis of AAV expression and optic fiber location

Viral expression and optic fiber location were verified *post hoc*, at the end of the experiments (**Fig. 8**). Mice were anesthetized with isoflurane (3-5%) and transcardially perfused with 4% paraformaldehyde (PFA) in 0.1 M sodium phosphate buffer (PBS). 50 µm-thick brain coronal sections were prepared using a DSK Microslicer (DTK-1000), stained with DAPI (1:1000) to label cell nuclei, and mounted with Prolong diamond antifade reagent montant (ThermoFisher) onto microscope slides. Zeiss LSM 880 Airyscan Confocal microscope with Super-Resolution and ZEN (black edition) software and a 25X oil-immersion objective were used for images acquisition.

Quantification and Statistical Analysis

The normality of distributions was assessed using the Shapiro-Wilk test. In normal distributions, Student's unpaired and paired two-tailed t tests were used to assess between-group and within-group differences, respectively. One way ANOVA and One way ANOVA repeated measure (RM) were used when more than two groups were compared.

The non-parametric paired sample Wilcoxon signed rank test and Mann-Whitney's U test were used in non-normal distributions. Statistical significance was set to $p < 0.05$ (*** indicates $p < 0.001$, ** indicates $p < 0.01$, and * indicates $p < 0.05$). All values are reported as the mean ± SEM. Statistical results are summarized in **Table S1**. All experiments included at least three animals per condition. Statistical analysis was performed using OriginPro software (OriginLab).

Acknowledgments

We thank all the Castillo lab members for their invaluable feedback; Dr. Anita Autry Lab (Einstein) for sharing their photometry system and for technical support, especially to Ilaria Carta and Dr. Giovanni Podda; Subrina Persaud for assisting with confocal image acquisition; and Yulong Li (Peking University) for helpful discussions about the adenosine sensor. This work was supported by NIH grants R01 MH116673, R01MH125772, and R01 NS 113600 to P.E.C.. K.N. was partially supported by a Postdoctoral Research Fellowship (American Epilepsy Society), the Fondation pour la Recherche Médicale (postdoctoral fellowship for research abroad) and the Fondation Bettencourt Schueller (Prix pour les Jeunes Chercheurs 2016). Y.H. was supported by the Japan Society for the Promotion of Science postdoctoral fellowships for research abroad (H23.829). A.E.C. was partially supported by a Ruth L. Kirschstein Award (F32 NS071821), a NARSAD Young Investigator Grant from the Brain & Behavior Research Foundation, and by Chilean Fondecyt regular (#1201848). M.G. was supported by a Ruth L. Kirschestein (F31MH122134). R.L. was funded by the Spanish Ministerio de Economia y Competitividad (RTI2018-095812-B-I00) and Junta de Comunidades de Castillo-La Mancha (SBPLY/17/180501/000229). Confocal images were obtained at the Einstein Imaging Core (supported by The Rose F Kennedy Intellectual Disabilities Research Center - shared instrument grant 1S10OD25295 to Konstantin Dobrenis).

Conflict of interest

Authors declare no conflict of interest.

Author contributions

K.N. and P.E.C. designed studies and wrote the manuscript. K.N. performed experiments and analyzed all data except for the *in vitro* adenosine measurements that were designed, performed, and analyzed by C.B.. R.L. performed and analyzed immunoelectron microscopy experiments. M.G. tested the role of A1 receptors. Y.H and A.C designed, performed, and analyzed early experiments assessing conventional retrograde signals. All authors read and edited the manuscript.

REFERENCES

1 Lisman, J. E. Relating hippocampal circuitry to function: recall of memory sequences by reciprocal dentate-CA3 interactions. *Neuron* **22**, 233-242, doi:10.1016/s0896-6273(00)81085-5 (1999).

2 Scharfman, H. E. The enigmatic mossy cell of the dentate gyrus. *Nat Rev Neurosci* **17**, 562-575, doi:10.1038/nrn.2016.87 (2016).

3 Jinde, S., Zsiros, V. & Nakazawa, K. Hilar mossy cell circuitry controlling dentate granule cell excitability. *Front Neural Circuits* **7**, 14, doi:10.3389/fncir.2013.00014 (2013).

4 Scharfman, H. E. & Myers, C. E. Hilar mossy cells of the dentate gyrus: a historical perspective. *Front Neural Circuits* **6**, 106, doi:10.3389/fncir.2012.00106 (2012).

5 Ratzliff, A., Santhakumar, V., Howard, A. & Soltesz, I. Mossy cells in epilepsy: rigor mortis or vigor mortis? *Trends Neurosci* **25**, 140-144, doi:10.1016/s0166-2236(00)02122-6 (2002).

6 Hashimotodani, Y. *et al.* LTP at Hilar Mossy Cell-Dentate Granule Cell Synapses Modulates Dentate Gyrus Output by Increasing Excitation/Inhibition Balance. *Neuron* **95**, 928-943 e923, doi:10.1016/j.neuron.2017.07.028 (2017).

7 Berthoux, C., Nasrallah, K. & Castillo, P. E. BDNF-induced BDNF release mediates long-term potentiation *(in preparation)* (2021).

8 Nasrallah, K. *et al.* Activity-dependent LTP in the dentate gyrus promotes epileptic seizures. *https://www.biorxiv.org/content/10.1101/2021.06.30.450628v1* (2021).

9 Castillo, P. E. Presynaptic LTP and LTD of excitatory and inhibitory synapses. *Cold Spring Harb Perspect Biol* **4**, doi:10.1101/cshperspect.a005728 (2012).

10 Regehr, W. G., Carey, M. R. & Best, A. R. Activity-dependent regulation of synapses by retrograde messengers. *Neuron* **63**, 154-170, doi:10.1016/j.neuron.2009.06.021 (2009).

11 Younts, T. J., Chevaleyre, V. & Castillo, P. E. CA1 pyramidal cell theta-burst firing triggers endocannabinoid-mediated long-term depression at both somatic and dendritic inhibitory synapses. *J Neurosci* **33**, 13743-13757, doi:10.1523/JNEUROSCI.0817-13.2013 (2013).

12 Chiu, C. Q. & Castillo, P. E. Input-specific plasticity at excitatory synapses mediated by endocannabinoids in the dentate gyrus. *Neuropharmacology* **54**, 68-78, doi:10.1016/j.neuropharm.2007.06.026 (2008).

13 Shimojo, M. *et al.* SNAREs Controlling Vesicular Release of BDNF and Development of Callosal Axons. *Cell Rep* **11**, 1054-1066, doi:10.1016/j.celrep.2015.04.032 (2015).

14 Jensen, K. R., Berthoux, C., Nasrallah, K. & Castillo, P. E. Multiple cannabinoid signaling cascades powerfully suppress recurrent excitation in the hippocampus. *Proc Natl Acad Sci U S A* **118**, doi:10.1073/pnas.2017590118 (2021).

15 Williams, J. H. *et al.* The suppression of long-term potentiation in rat hippocampus by inhibitors of nitric oxide synthase is temperature and age dependent. *Neuron* **11**, 877-884, doi:10.1016/0896-6273(93)90117-a (1993).

16 Chevaleyre, V. & Castillo, P. E. Heterosynaptic LTD of hippocampal GABAergic synapses: a novel role of endocannabinoids in regulating excitability. *Neuron* **38**, 461-472, doi:10.1016/s0896-6273(03)00235-6 (2003).

17 Sebastiao, A. M. & Ribeiro, J. A. Triggering neurotrophic factor actions through adenosine A2A receptor activation: implications for neuroprotection. *Br J Pharmacol* **158**, 15-22, doi:10.1111/j.1476-5381.2009.00157.x (2009).

18 Diogenes, M. J., Fernandes, C. C., Sebastiao, A. M. & Ribeiro, J. A. Activation of adenosine A2A receptor facilitates brain-derived neurotrophic factor modulation of synaptic transmission in hippocampal slices. *J Neurosci* **24**, 2905-2913, doi:10.1523/JNEUROSCI.4454-03.2004 (2004).

19 Fontinha, B. M., Diogenes, M. J., Ribeiro, J. A. & Sebastiao, A. M. Enhancement of long-term potentiation by brain-derived neurotrophic factor requires adenosine A2A receptor activation by endogenous adenosine. *Neuropharmacology* **54**, 924-933, doi:10.1016/j.neuropharm.2008.01.011 (2008).

20 Latini, S. & Pedata, F. Adenosine in the central nervous system: release mechanisms and extracellular concentrations. *J Neurochem* **79**, 463-484, doi:10.1046/j.1471-4159.2001.00607.x (2001).

21 King, A. E., Ackley, M. A., Cass, C. E., Young, J. D. & Baldwin, S. A. Nucleoside transporters: from scavengers to novel therapeutic targets. *Trends Pharmacol Sci* **27**, 416-425, doi:10.1016/j.tips.2006.06.004 (2006).

22 Lovatt, D. *et al.* Neuronal adenosine release, and not astrocytic ATP release, mediates feedback inhibition of excitatory activity. *Proc Natl Acad Sci U S A* **109**, 6265-6270, doi:10.1073/pnas.1120997109 (2012).

23 Wall, M. J. & Dale, N. Neuronal transporter and astrocytic ATP exocytosis underlie activity-dependent adenosine release in the hippocampus. *J Physiol* **591**, 3853-3871, doi:10.1113/jphysiol.2013.253450 (2013).

24 Pons-Bennaceur, A. *et al.* Diadenosine-Polyphosphate Analogue AppCH2ppA Suppresses Seizures by Enhancing Adenosine Signaling in the Cortex. *Cereb Cortex* **29**, 3778-3795, doi:10.1093/cercor/bhy257 (2019).

25 Rebola, N., Lujan, R., Cunha, R. A. & Mulle, C. Adenosine A2A receptors are essential for long-term potentiation of NMDA-EPSCs at hippocampal mossy fiber synapses. *Neuron* **57**, 121-134, doi:10.1016/j.neuron.2007.11.023 (2008).

26 Atwood, B. K., Lovinger, D. M. & Mathur, B. N. Presynaptic long-term depression mediated by Gi/o-coupled receptors. *Trends Neurosci* **37**, 663-673, doi:10.1016/j.tins.2014.07.010 (2014).

27 Peng, W. *et al.* Regulation of sleep homeostasis mediator adenosine by basal forebrain glutamatergic neurons. *Science* **369**, doi:10.1126/science.abb0556 (2020).

28 Henze, D. A., Wittner, L. & Buzsaki, G. Single granule cells reliably discharge targets in the hippocampal CA3 network in vivo. *Nat Neurosci* **5**, 790-795, doi:10.1038/nn887 (2002).

29 Pernia-Andrade, A. J. & Jonas, P. Theta-gamma-modulated synaptic currents in hippocampal granule cells in vivo define a mechanism for network oscillations. *Neuron* **81**, 140-152, doi:10.1016/j.neuron.2013.09.046 (2014).

30 Diamantaki, M., Frey, M., Berens, P., Preston-Ferrer, P. & Burgalossi, A. Sparse activity of identified dentate granule cells during spatial exploration. *Elife* **5**, doi:10.7554/eLife.20252 (2016).

31 GoodSmith, D. *et al.* Spatial Representations of Granule Cells and Mossy Cells of the Dentate Gyrus. *Neuron* **93**, 677-690 e675, doi:10.1016/j.neuron.2016.12.026 (2017).

32 Senzai, Y. & Buzsaki, G. Physiological Properties and Behavioral Correlates of Hippocampal Granule Cells and Mossy Cells. *Neuron* **93**, 691-704 e695, doi:10.1016/j.neuron.2016.12.011 (2017).

33 Danielson, N. B. *et al.* In Vivo Imaging of Dentate Gyrus Mossy Cells in Behaving Mice. *Neuron* **93**, 552-559 e554, doi:10.1016/j.neuron.2016.12.019 (2017).

34 Nahir, B., Bhatia, C. & Frazier, C. J. Presynaptic inhibition of excitatory afferents to hilar mossy cells. *J Neurophysiol* **97**, 4036-4047, doi:10.1152/jn.00069.2007 (2007).

35 Hedrick, T. P. *et al.* Excitatory Synaptic Input to Hilar Mossy Cells under Basal and Hyperexcitable Conditions. *eNeuro* **4**, doi:10.1523/ENEURO.0364-17.2017 (2017).

36 Leschik, J. *et al.* Prominent Postsynaptic and Dendritic Exocytosis of Endogenous BDNF Vesicles in BDNF-GFP Knock-in Mice. *Mol Neurobiol* **56**, 6833-6855, doi:10.1007/s12035-019-1551-0 (2019).

37 Ribeiro, J. A. & Sebastiao, A. M. On the role, inactivation and origin of endogenous adenosine at the frog neuromuscular junction. *J Physiol* **384**, 571-585, doi:10.1113/jphysiol.1987.sp016470 (1987).

38 Zimmermann, H. Ectonucleotidases in the nervous system. *Novartis Found Symp* **276**, 113-128; discussion 128-130, 233-117, 275-181 (2006).

39 Wall, M. & Dale, N. Activity-dependent release of adenosine: a critical re-evaluation of mechanism. *Curr Neuropharmacol* **6**, 329-337, doi:10.2174/157015908787386087 (2008).

40 Arch, J. R. & Newsholme, E. A. Activities and some properties of 5'-nucleotidase, adenosine kinase and adenosine deaminase in tissues from vertebrates and invertebrates in relation to the control of the concentration and the physiological role of adenosine. *Biochem J* **174**, 965-977, doi:10.1042/bj1740965 (1978).

41 Lee, F. S. & Chao, M. V. Activation of Trk neurotrophin receptors in the absence of neurotrophins. *Proc Natl Acad Sci U S A* **98**, 3555-3560, doi:10.1073/pnas.061020198 (2001).

42 Correia-de-Sa, P., Sebastiao, A. M. & Ribeiro, J. A. Inhibitory and excitatory effects of adenosine receptor agonists on evoked transmitter release from phrenic nerve ending of the rat. *Br J Pharmacol* **103**, 1614-1620, doi:10.1111/j.1476-5381.1991.tb09836.x (1991).

43 Pousinha, P. A., Diogenes, M. J., Ribeiro, J. A. & Sebastiao, A. M. Triggering of BDNF facilitatory action on neuromuscular transmission by adenosine A2A receptors. *Neurosci Lett* **404**, 143-147, doi:10.1016/j.neulet.2006.05.036 (2006).

44 Dixon, A. K., Gubitz, A. K., Sirinathsinghji, D. J., Richardson, P. J. & Freeman, T. C. Tissue distribution of adenosine receptor mRNAs in the rat. *Br J Pharmacol* **118**, 1461-1468, doi:10.1111/j.1476-5381.1996.tb15561.x (1996).

45 Dias, R. B., Rombo, D. M., Ribeiro, J. A., Henley, J. M. & Sebastiao, A. M. Adenosine: setting the stage for plasticity. *Trends Neurosci* **36**, 248-257, doi:10.1016/j.tins.2012.12.003 (2013).

46 Duster, R., Prickaerts, J. & Blokland, A. Purinergic signaling and hippocampal long-term potentiation. *Curr Neuropharmacol* **12**, 37-43, doi:10.2174/1570159X113119990045 (2014).

47 Pousinha, P. A., Correia, A. M., Sebastiao, A. M. & Ribeiro, J. A. Predominance of adenosine excitatory over inhibitory effects on transmission at the neuromuscular junction of infant rats. *J Pharmacol Exp Ther* **332**, 153-163, doi:10.1124/jpet.109.157255 (2010).

48 Correia-de-Sa, P., Timoteo, M. A. & Ribeiro, J. A. Presynaptic A1 inhibitory/A2A facilitatory adenosine receptor activation balance depends on motor nerve stimulation paradigm at the rat hemidiaphragm. *J Neurophysiol* **76**, 3910-3919, doi:10.1152/jn.1996.76.6.3910 (1996).

49 Sebastiao, A. M. & Ribeiro, J. A. Adenosine receptors and the central nervous system. *Handb Exp Pharmacol*, 471-534, doi:10.1007/978-3-540-89615-9_16 (2009).

50 Alzheimer, C., Rohrenbeck, J. & ten Bruggencate, G. Adenosine depresses induction of LTP at the mossy fiber-CA3 synapse in vitro. *Brain Res* **543**, 163-165, doi:10.1016/0006-8993(91)91061-5 (1991).

51 Forghani, R. & Krnjevic, K. Adenosine antagonists have differential effects on induction of long-term potentiation in hippocampal slices. *Hippocampus* **5**, 71-77, doi:10.1002/hipo.450050109 (1995).

52 Bui, A. D. *et al.* Dentate gyrus mossy cells control spontaneous convulsive seizures and spatial memory. *Science* **359**, 787-790, doi:10.1126/science.aan4074 (2018).

53 Fredes, F. *et al.* Ventro-dorsal Hippocampal Pathway Gates Novelty-Induced Contextual Memory Formation. *Curr Biol* **31**, 25-38 e25, doi:10.1016/j.cub.2020.09.074 (2021).

54 Fontinha, B. M. *et al.* Adenosine A(2A) receptor modulation of hippocampal CA3-CA1 synapse plasticity during associative learning in behaving mice. *Neuropsychopharmacology* **34**, 1865-1874, doi:10.1038/npp.2009.8 (2009).

55 Wei, C. J. *et al.* Regulation of fear responses by striatal and extrastriatal adenosine A2A receptors in forebrain. *Biol Psychiatry* **75**, 855-863, doi:10.1016/j.biopsych.2013.05.003 (2014).

56 Beamer, E., Kuchukulla, M., Boison, D. & Engel, T. ATP and adenosine-Two players in the control of seizures and epilepsy development. *Prog Neurobiol* **204**, 102105, doi:10.1016/j.pneurobio.2021.102105 (2021).

57 El Yacoubi, M., Ledent, C., Parmentier, M., Costentin, J. & Vaugeois, J. M. Evidence for the involvement of the adenosine A(2A) receptor in the lowered susceptibility to pentylenetetrazol-induced seizures produced in mice by long-term treatment with caffeine. *Neuropharmacology* **55**, 35-40, doi:10.1016/j.neuropharm.2008.04.007 (2008).

58 El Yacoubi, M., Ledent, C., Parmentier, M., Costentin, J. & Vaugeois, J. M. Adenosine A2A receptor deficient mice are partially resistant to limbic seizures. *Naunyn Schmiedebergs Arch Pharmacol* **380**, 223-232, doi:10.1007/s00210-009-0426-8 (2009).

59 Jones, P. A., Smith, R. A. & Stone, T. W. Protection against hippocampal kainate excitotoxicity by intracerebral administration of an adenosine A2A receptor antagonist. *Brain Res* **800**, 328-335, doi:10.1016/s0006-8993(98)00540-x (1998).

60 Lee, H. K., Choi, S. S., Han, K. J., Han, E. J. & Suh, H. W. Roles of adenosine receptors in the regulation of kainic acid-induced neurotoxic responses in mice. *Brain Res Mol Brain Res* **125**, 76-85, doi:10.1016/j.molbrainres.2004.03.004 (2004).

61 Rosim, F. E. *et al.* Differential neuroprotection by A(1) receptor activation and A(2A) receptor inhibition following pilocarpine-induced status epilepticus. *Epilepsy Behav* **22**, 207-213, doi:10.1016/j.yebeh.2011.07.004 (2011).

62 Fukuda, M., Suzuki, Y., Hino, H., Morimoto, T. & Ishii, E. Activation of central adenosine A(2A) receptors lowers the seizure threshold of hyperthermia-induced seizure in childhood rats. *Seizure* **20**, 156-159, doi:10.1016/j.seizure.2010.11.012 (2011).

63 Sandau, U. S. *et al.* Adenosine Kinase Deficiency in the Brain Results in Maladaptive Synaptic Plasticity. *J Neurosci* **36**, 12117-12128, doi:10.1523/JNEUROSCI.2146-16.2016 (2016).

64 McNamara, J. O. & Scharfman, H. E. in *Jasper's Basic Mechanisms of the Epilepsies* (eds th *et al.*) (2012).

65 Botterill, J. J. *et al.* An Excitatory and Epileptogenic Effect of Dentate Gyrus Mossy Cells in a Mouse Model of Epilepsy. *Cell Rep* **29**, 2875-2889 e2876, doi:10.1016/j.celrep.2019.10.100 (2019).

66 Lujan, R., Nusser, Z., Roberts, J. D., Shigemoto, R. & Somogyi, P. Perisynaptic location of metabotropic glutamate receptors mGluR1 and mGluR5 on dendrites and dendritic spines in the rat hippocampus. *Eur J Neurosci* **8**, 1488-1500, doi:10.1111/j.1460-9568.1996.tb01611.x (1996).

FIGURE LEGENDS

Figure 1: Theta-burst firing of a single postsynaptic GC induces presynaptic LTP at MC-GC synapse

(a) *Left,* Diagram illustrating the recording configuration. MC and MPP EPSCs were recorded from the same GC and evoked with stimulation electrodes placed in the inner and middle molecular layer, respectively. *Right*, Current clamp recording showing GC theta-burst firing (GC TBF). LTP induction protocol (GC TBF) was composed of 10 bursts at 5 Hz of 5 action potentials at 50 Hz, repeated 4 time every 5 s.

(b) *Left,* Representative traces before (1) and after (2) GC TBF delivery. *Right,* Time-course plot showing that GC TBF induced LTP at MC-GC but not at MPP-GC synapses.

(c) GC TBF-induced LTP was associated with significant reduction in PPR and CV (n = 13 cells).

(d) LTP was blocked when TrkB was conditionally knocked out from from GCs (Post TrkB cKO, *TrkB*$^{fl/fl}$ mice injected with AAV5.CaMKII.Cre.GFP). LTP was unaffected in control animals (Control, *TrkB*$^{fl/fl}$ mice injected with AAV5.CaMKII.eGFP).

(e) LTP was normally induced when loading PKI_{6-22} (2.5 µM) in GCs via the recording pipette but completely blocked when the cell-permeant PKA inhibitor PKI_{14-22} myristoylated (1 µM) was bath applied.

(f) Summary bar graph showing the magnitude of GC TBF induced LTP in the presence of DGC-IV (1 µM), when TrkB was conditionally knocked out from MCs (Pre TrkB cKO), when loading the PKI_{6-22} (2.5 µM) in GCs and in presence of D-APV (50 µM). LTP was abolished in presence of the TrkB antagonist ANA-12 (15 µM), Botox (0.5 µM loaded postsynaptically), postsynaptic BDNF and TrkB cKO, and bath application of the PKA inhibitors H89 (10 µM) or PKI_{14-22} myristoylated (1 µM).

Numbers in parentheses indicate the number of cells. Data are presented as mean ± SEM.

Figure 2: MC-GC LTP does not require conventional retrograde messengers

(a) Bath application of the NO synthase inhibitor L-NAME (100 µM, 50- to 90-min pre-incubation and bath applied) did not impair MC-GC LTP.

(b) Positive controls for L-NAME. Extracellular recordings in CA1 *stratum radiatum*

showing that L-NAME blocked LTP at SC-CA1 synapses induced by 4 HFS (100 pulses at 100 Hz repeated 4 times every 10 s) at 25 °C.

(c) Application of cocktail of lipase inhibitors AACOCF3 (10 μM, 50- to 90-min pre-incubation and bath applied), Baicalein (3 μM, 50- to 90-min pre-incubation and bath applied), and THL (4 μM loaded in the recording pipette) did not affect MC-GC LTP.

(d) Positive controls for AACOCF3 and Baicalein. Extracellular recordings in CA1 *stratum radiatum* showing that application of AACOCF3 and Baicalein significantly reduced LFS (900 pulses at 1 Hz)-induced LTD at SC-CA1 synapses.

(e) Positive control for the lipase inhibitor THL showing that loading THL in CA1 pyramidal neuron via the recording pipette blocked iLTD induced by TBS (10 bursts at 5 Hz of 5 pulses at 100 Hz, repeated every 5 s, 4 times).

Numbers in parentheses represent number of cells. Data are presented as mean ± SEM.

Figure 3: MC-GC LTP requires activation of presynaptic A_{2A}Rs whereas A_1Rs dampen LTP.

(a) Bath application of the A_{2A}R selective antagonists SCH 58261 (100 nM) and ZM241385 (50 nM) blocked GC TBF-induced LTP.

(b) SCH 58261 (100 nM) did not change basal EPSC amplitude.

(c) SCH 58261 (100 nM) abolished LTP induced by BDNF puffs (8 nm, 2 puffs of 3 s in the IML), as compared with interleaved controls.

(d) *Left,* loading GDPβS in the recording pipette did not affect MC-GC LTP. *Right*, positive control showing that replacing GTP by 1 mM GDPβS in the internal solution efficiently abolished the $GABA_B$ receptor agonist (baclofen, 10 μM)-induced increase in holding current.

(e, f) Presynaptic A_{2A}R cKO abolished MC-GC LTP. **(e)** *Left,* **A mix of** AAV5.CamKII.Cre-mCherry and AAV_{DJ}.hSyn.Flex.ChIEF.Tdtomato was injected unilaterally into the DG of $A_{2A}R^{fl/fl}$ (cKO) or WT (control) mice. MC EPSCs were light-evoked and recorded in contralateral DG. *Right,* Infrared/differential interference contrast (IR/DIC, left images) and fluorescence (right) images showing that ChIEF-TdTomato was expressed in MC soma in ipsilateral DG (top) and selectively in putative MC axons (bottom) of contralateral IML. **(f)** MC-GC LTP was abolished in presynaptic A_{2A}R conditional knockout mice as compared

977 with controls.

978 **(g)** MC-GC LTP magnitude was increased in the presence of the A_1R selective antagonist
979 DPCPX (100 nM) as compared to interleaved control experiments.

980 **(h)** Application of DPCPX (100 nM) did not change basal EPSC amplitude at MC-GC and
981 MPP-GC synapses.

982 Numbers in parentheses represent number of cells. Data are presented as mean ± SEM.

983
984 **Figure 4: Subcellular localization of the A_1 and A_{2A} adenosine receptors in the**
985 **molecular layer of the dentate gyrus.**
986
987 **(a-c, e-g)** Electron micrographs of the molecular layer of the dentate gyrus showing
988 immunoreactivity for A_1Rs and $A_{2A}Rs$ revealed by pre-embedding immunogold methods.

989 **(a-c)** Both at MC-GC **(a and b)** and PP-GC **(c)** putative synapses, immunoparticles for
990 A_1R were mainly observed on the presynaptic plasma membrane (arrowheads) of axon
991 terminals (at), with very low frequency in postsynaptic sites (arrows) of spines (s) or
992 dendritic shafts (Den).

993 **(d)** Quantitative analysis of the relative number of immunoparticles found in the
994 presynaptic membrane for A_1R at MC-GC and MPP-GC putative synapses. From the total
995 number of immunoparticles detected (n = 490 for MC-GC; n = 419 for MPP-GC synapses,
996 N = 3 mice), 468 (95.5%) and 402 (95.9%) were present in presynaptic sites of MC-GC
997 and MPP-GC putative synapses, respectively.

998 **(e-h)** Electron micrographs **(e-g)** and quantitative analysis **(h)** showing that, at putative
999 MC-GC synapses **(e, f and h)**, immunoparticles for $A_{2A}R$ were mainly detected
1000 presynaptically (91.0%) whereas they were mainly found on the postsynaptic plasma
1001 membrane (92.0%) of putative PP-GC synapses **(g and h)**. Total number of
1002 immunoparticles: n = 668 for MC-GC; n = 690 for MPP-GC synapses, N = 3 mice.

1003 Scale bars: 200 nm.

1004

1005 **Figure 5: $A_{2A}R$ activation is sufficient to trigger PKA-dependent LTP at MC-GC but**
1006 **not at MPP-GC synapses.**

1007 **(a)** Representative traces *(left)* and time-course summary plot *(right)* showing that bath
1008 application of the $A_{2A}R$ selective agonist CGS21680 (50 nM) potentiated MC-GC but not

MPP-GC synaptic transmission.

(b) CGS21680-induced potentiation at MC-GC synapse was associated with a significant reduction of both PPR and CV. ** $p < 0.01$; n = 9 cells.

(c) CGS21680 induced long-lasting potentiation even when the $A_{2A}R$ selective antagonist SCH 58261 (100 nM) was included during CGS21680 washout. CGS21680-induced LTP was completely abolished in continuous presence of SCH 58261.

(d) Loading the selective PKA blocker PKI_{6-22} (2.5 μM) in GCs via the recording pipette did not impair CGS21680-induced LTP while bath application of the cell-permeant PKA inhibitor PKI_{14-22} myristoylated (1 μM) completely blocked LTP.

(e) Bath application of ANA-12 (15 μM) did not impair CGS21680-induced LTP.

(f) Positive control in interleaved experiments showing that ANA-12 (15 μM) efficiently blocked GC TBF-induced LTP.

Numbers in parentheses represent number of cells. Data are presented as mean ± SEM.

Figure 6: MC-GC LTP requires passive release of adenosine from GCs, via ENTs.

(a) Representative traces *(left)* and time-course summary plot *(right)* showing that GC TBF failed to induce LTP in presence of the ENT blockers (20 μM of dipyridamole and 10 μM of NBMPR) as compared with interleaved controls.

(b) Bath application of the ENT blockers (20 μM of dipyridamole and 10 μM of NBMPR) did not change basal MC-GC EPSC amplitude.

(c) Co-application of the ENT blockers (20 μM of dipyridamole and 10 μM of NBMPR) and the A_1R antagonist DPCPX (100 nM) increased EPSC amplitude in control condition but not in presence of the $A_{2A}R$ antagonist SCH 58261 (100 nM).

(d) Including inosine (100 μM) in the recording solution completely prevented GC TBF-induced LTP.

(e) Bath application of inosine (100 μM) did not change basal MC-GC EPSC amplitude.

(f) Bath application of DPCPX (100 nM) increased EPSC amplitude when the ENT blockers (20 μM of dipyridamole and 10 μM of NBMPR) were included in the bath but not when inosine (100 μM) was loaded in the postsynaptic neuron *via* the patch pipette.

Numbers in parentheses represent number of cells. Data are represented as mean ± SEM.

Figure 7: Induction of MC-GC LTP triggers a transient TrkB-dependent increase in extracellular adenosine level

(a) AAV9.hSyn.GRAB.Ado1.0m ($GRAB_{Ado}$) was injected unilaterally in the DG of WT mice. Two-photon image (*bottom*) showing $GRAB_{Ado}$ was selectively expressed in putative MC axons in contralateral IML.

(b, c) Two-photon images **(b)** showing $GRAB_{Ado}$ fluorescence intensity increased during burst electrical stimulation of MC axon terminals (MC BS) in normal ACSF (control) but not in the presence of A_{2A} receptor antagonist SCH58261 (100 nM). Time-course summary plot of the average fractional fluorescence changes ($\Delta F/F_0$) with time are shown in **c**.

(d, e) Two-photon images **(d)** and time-course summary plot **(e)** showing how MC BS failed to increase $GRAB_{Ado}$ fluorescence in presence of the TrkB receptor antagonist ANA-12 (15 µM) or when TrkB was conditionally knocked out from GCs (Post TrkB cKO).

(f) Quantification of the averaged responses during burst stimulation of MCs (15-25 s) * $p < 0.05$, ** $p < 0.01$, *** $p < 0.001$; one-way ANOVA.

Number of slices are shown between parentheses. Data are represented as mean ± SEM.

Figure 8: *In vivo* release of adenosine during epileptic seizures likely promotes seizures by activating A_{2A}Rs

(a) AAV9.hSyn.GRAB.Ado1.0m ($GRAB_{Ado}$) was injected unilaterally in the DG of WT mice. An optic fiber was implanted above the contralateral IML. Fiber photometry was performed 3-5 weeks later to assess $GRAB_{Ado}$ fluorescence intensity before and after acute seizure induction with kainic acid (KA, 30 mg/kg).

(b) Confocal image showing fiber tract and $GRAB_{Ado}$ expression in the contralateral IML.

(c, d) Time-course of representative experiment **(c)** and histogram **(d)** showing how KA (30 mg/kg) administration increased the average fractional fluorescence ($\Delta F/F_0$) of $GRAB_{Ado}$. * $p < 0.05$, $n = 5$, paired t test.

(e) Representation of the experimental timeline. AAV5-CaMKII-Cre-mCherry was injected bilaterally into ventral and dorsal DG of WT (control) and $A_{2A}R^{fl/fl}$ (cKO) mice. Mouse behavior was assessed for 120 min following KA (20 mg/kg) administration.

(f) Confocal images showing the viral expression in the DG of WT (top) and $A_{2A}R^{fl/fl}$ (bottom) mice.

(g-i) Deletion of $A_{2A}R$ from DG excitatory neurons ($A_{2A}R$ cKO, $A_{2A}R^{fl/fl}$ mice injected with AAV_5-CaMKII-Cre-mCherry) significantly increased latency to convulsive seizures **(g, h)** but did not affect seizure severity **(i).** ** $p < 0.01$, unpaired t test.

Numbers in parentheses represent number of mice. Data are presented as mean ± SEM.

SUPPLEMENTAL FIGURE LEGENDS

Figure_S1 (related to Figure 1): GC TBF-induced LTP properties

(a) GC TBF induced a normal LTP in presence of the group II mGluR agonist DCG-IV (1 µM) as compared to interleaved controls.

(b) TBF-induced LTP was blocked in presence of the TrkB selective antagonist ANA-12.

(c) Presynaptic TrkB cKO did not impair GC TBF-induced LTP. $TrkB^{fl/fl}$ mice were unilaterally injected with a mix of AAV_5.CaMKII.Cre and AAV_{DJ}.hSyn.Flex.ChiEF.Tdtomato. EPSCs were recorded in contralateral DG in response to light stimulation of Cre+ and ChIEF+ MC axons (lacking TrkB).

(d) GC TBF-induced LTP was blocked in GFP-Cre+ GCs (BDNF cKO, $Bdnf^{fl/fl}$ mice injected with AAV_5.CaMKII.Cre.GFP) as compared with GFP+ GCs (control, $Bdnf^{fl/fl}$ mice injected with AAV_5.CaMKII.eGFP).

(e) Loading Botox (0.5 µM) in the postsynaptic neuron via the patch pipette completely abolished MC-GC LTP.

(f) GC TBF failed to induce LTP in presence of the PKA inhibitor H89 (10 µM, 40- to 60 min pre-incubation and bath applied, black circles).

(g) Bath application of the selective NMDAR antagonist D-APV (50 µM, black circles) did not affect GC TBF-induced LTP, as compared with interleaved control experiments (white circles). Representative traces are shown on the left and time-course summary plot on the right.

Numbers in parentheses represent number of cells. Data are presented as mean ± SEM.

Figure_S2 (related to Figure 1): GC TBF- and MC BS-induced LTP occlude each

other

(a) Representative single cell experiments showing how GC TBF induced a normal LTP in naive slices (top) but not when MC BS was previously applied (bottom). Vertical dashed line indicated the time point when stimulation intensity was reduced in order to avoid potential ceiling effect.

(b) Representative traces and time course summary plot showing how MC BS occluded GC TBF -induced LTP.

(c) Representative single cell experiments showing how MC BS induced a normal LTP in naive slices (top) but not when GC TBF was previously applied (bottom). Vertical dashed line indicated the time point when stimulation intensity was reduced in order to avoid potential ceiling effect.

(d) Pre-application of the GC TBF protocol occluded MC BS-induced LTP (black circles) as compared with interleaved controls (naive, white circles).

Numbers in parentheses represent number of cells. Data are presented as mean ± SEM.

Figure_S3 (related to Figure 2): MC-GC LTP does not require conventional retrograde messengers

MC BS induced a normal LTP in presence of L-NAME **(a)**, AACOCF3 **(b)**, Baicalein **(c)** or when THL was loaded **(d)** in the postsynaptic GC, as compared with interleaved controls.

Numbers in parentheses represent number of cells. Data are presented as mean ± SEM.

Figure S4 (related to fig 4): MC BS-induced LTP requires $A_{2A}R$ activation.

(a) Bath application of the $A_{2A}R$ selective antagonist SCH 58261 (100 nM) abolished LTP induced by MC BS (5 pulses at 100 Hz repeated 50 times every 0.5 s).

(b) *Left,* loading GDPβs (1 mM) in the recording pipette did not affect LTP induced by MC BS. *Right,* interleaved positive controls for $GDP_{\beta s}$ showing that replacing GTP by 1 mM $GDP_{\beta S}$ in the recording pipette abolished baclofen (10 µM)-induced increase in holding current. Baclofen is a $GABA_B$ receptor selective agonist.

Numbers in parentheses represent number of cells. Data are presented as mean ± SEM.

Figure_S5 (related to Figure 4): Activation of A1R induces a short-term depression

at both MC-GC and MPP-GC synapses

(a) Bath application of CCPA (50 nM, 15 min), a selective adenosine A_1R agonist, induced a short-term depression at both MC-GC and MPP-GC synapses. The selective A_1R antagonist DPCPX (100 nM) was included in the washout of CCPA.

(b, c) CCPA-induced depression was associated with a significant and reversible increase in both PPR and CV, *$p < 0.05$, $n = 7$, one-way ANOVA RM.

(d) Bath application of the A_1R antagonist DPCPX (100 nM) completely blocked CCPA-induced depression.

Numbers in parentheses represent number of cells. Data are presented as mean ± SEM.

Figure S6 (related to Figures 1-8). Adenosine is a retrograde messenger mediating activity-dependent presynaptic LTP at the MC-GC synapse

Scheme illustrating the emerging model for the mechanism of activity-induced MC-GC LTP. MC (MC BS) and GC bursts (GC TBF) of activity trigger BDNF release and subsequent TrkB activation in GCs (1). Activation of postsynaptic TrkB leads to intracellular accumulation of adenosine, which is passively released from GCs via ENTs (2). Adenosine then activates presynaptic A_1Rs and A_{2A}Rs (3). A_{2A}R activation induces a long-lasting PKA-dependent increase in glutamate (glu) release (4), whereas A_1R activation dampens LTP.

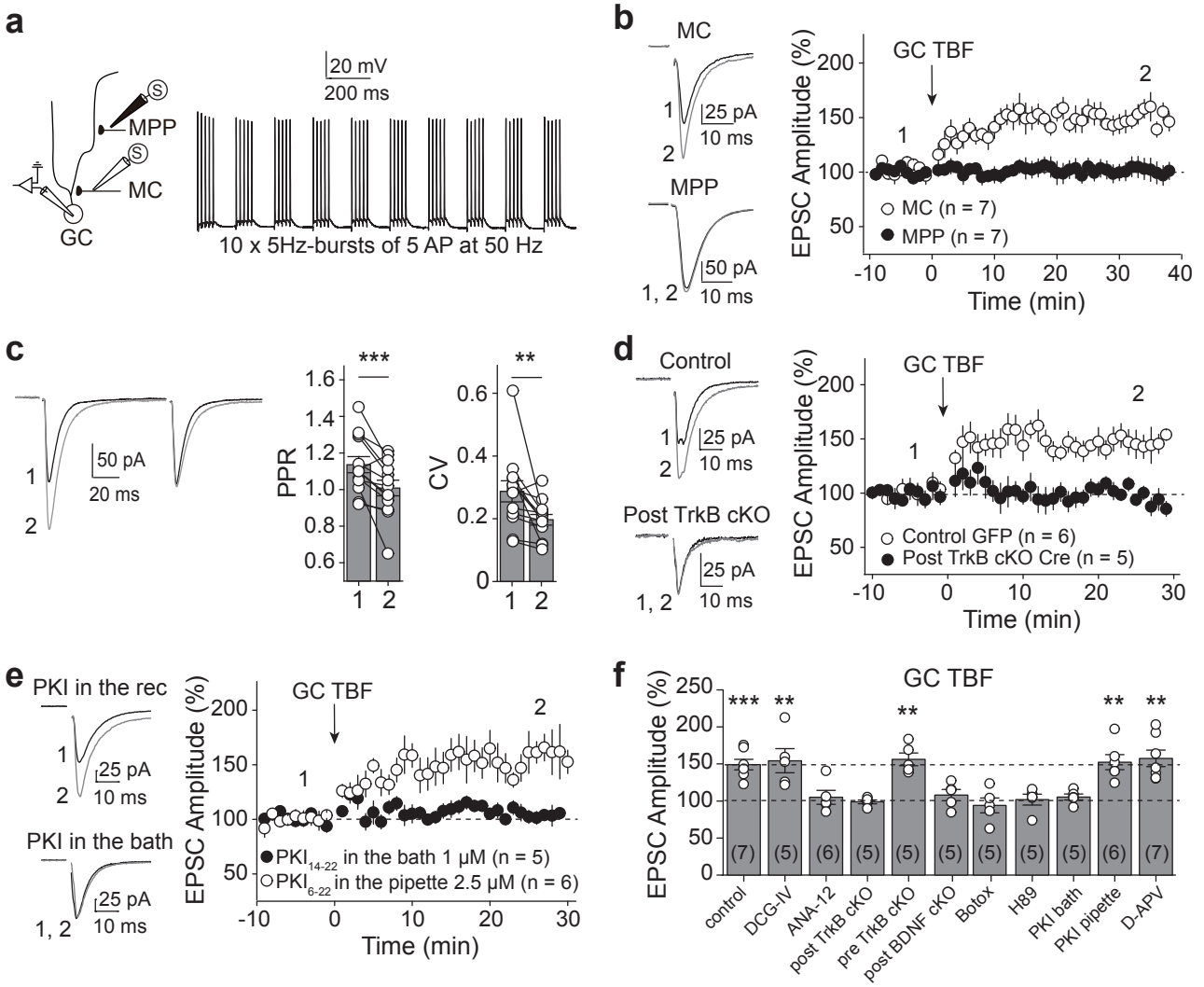
a
MPP
MC
GC
20 mV
200 ms
10 x 5Hz-bursts of 5 AP at 50 Hz
b
MC
MPP
25 pA
10 ms
50 pA
1, 2
GC TBF
EPSC Amplitude (%)
MC (n = 7)
MPP (n = 7)
Time (min)
c
50 pA
20 ms
PPR
CV
***
**
d
Control
Post TrkB cKO
Control GFP (n = 6)
Post TrkB cKO Cre (n = 5)
e
PKI in the rec
PKI in the bath
PKI14-22 in the bath 1 µM (n = 5)
PKI6-22 in the pipette 2.5 µM (n = 6)
f
control
DCG-IV
ANA-12
post TrkB cKO
pre TrkB cKO
post BDNF cKO
Botox
H89
PKI bath
PKI pipette
D-APV

Figure 1

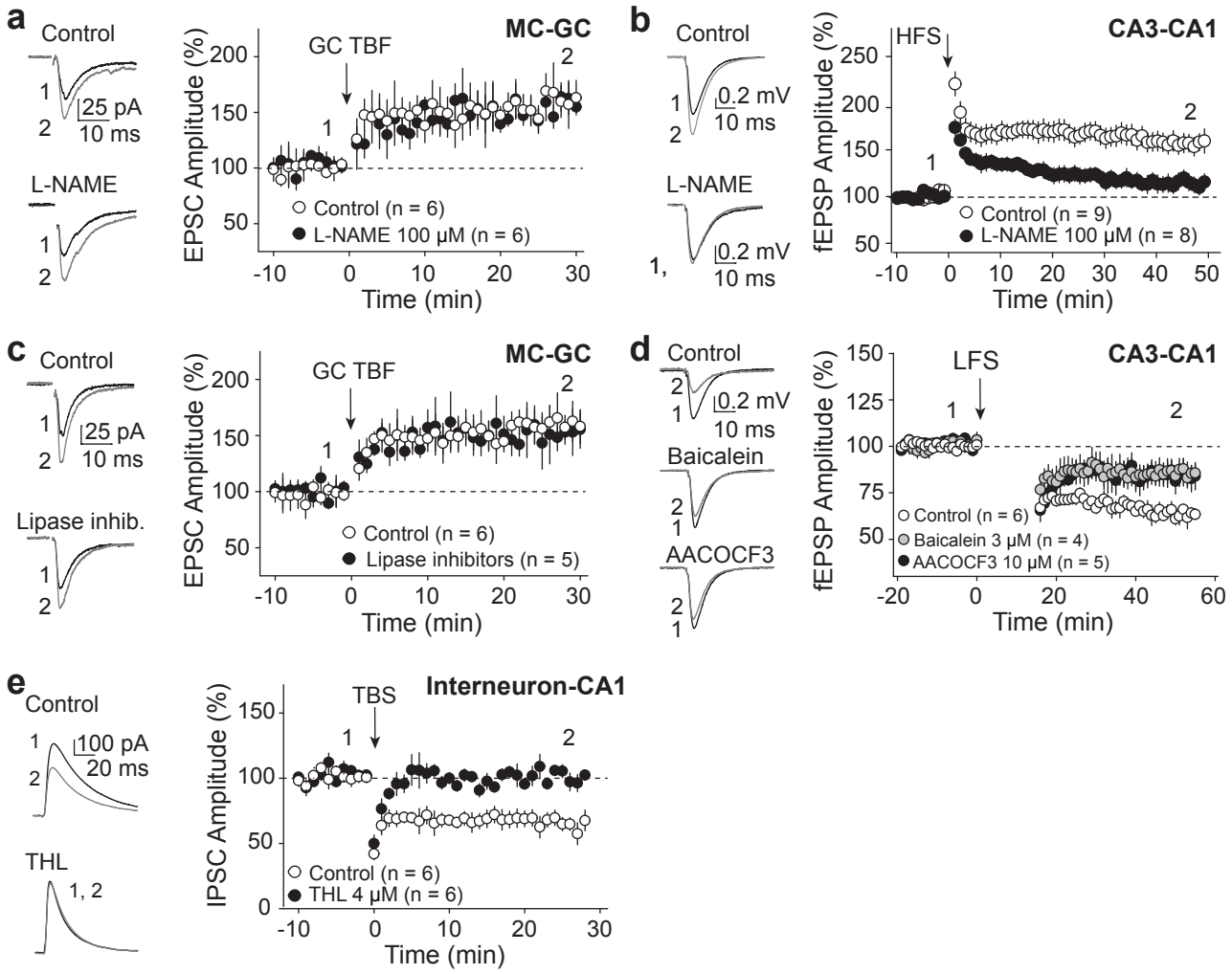
a
Control
25 pA
10 ms
L-NAME
MC-GC
GC TBF
EPSC Amplitude (%)
Control (n = 6)
L-NAME 100 µM (n = 6)
Time (min)
b
Control
0.2 mV
10 ms
L-NAME
CA3-CA1
HFS
fEPSP Amplitude (%)
Control (n = 9)
L-NAME 100 µM (n = 8)
Time (min)
c
Control
25 pA
10 ms
Lipase inhib.
MC-GC
GC TBF
EPSC Amplitude (%)
Control (n = 6)
Lipase inhibitors (n = 5)
Time (min)
d
Control
0.2 mV
10 ms
Baicalein
AACOCF3
CA3-CA1
LFS
fEPSP Amplitude (%)
Control (n = 6)
Baicalein 3 µM (n = 4)
AACOCF3 10 µM (n = 5)
Time (min)
e
Control
100 pA
20 ms
THL
1, 2
Interneuron-CA1
TBS
IPSC Amplitude (%)
Control (n = 6)
THL 4 µM (n = 6)
Time (min)

Figure 2

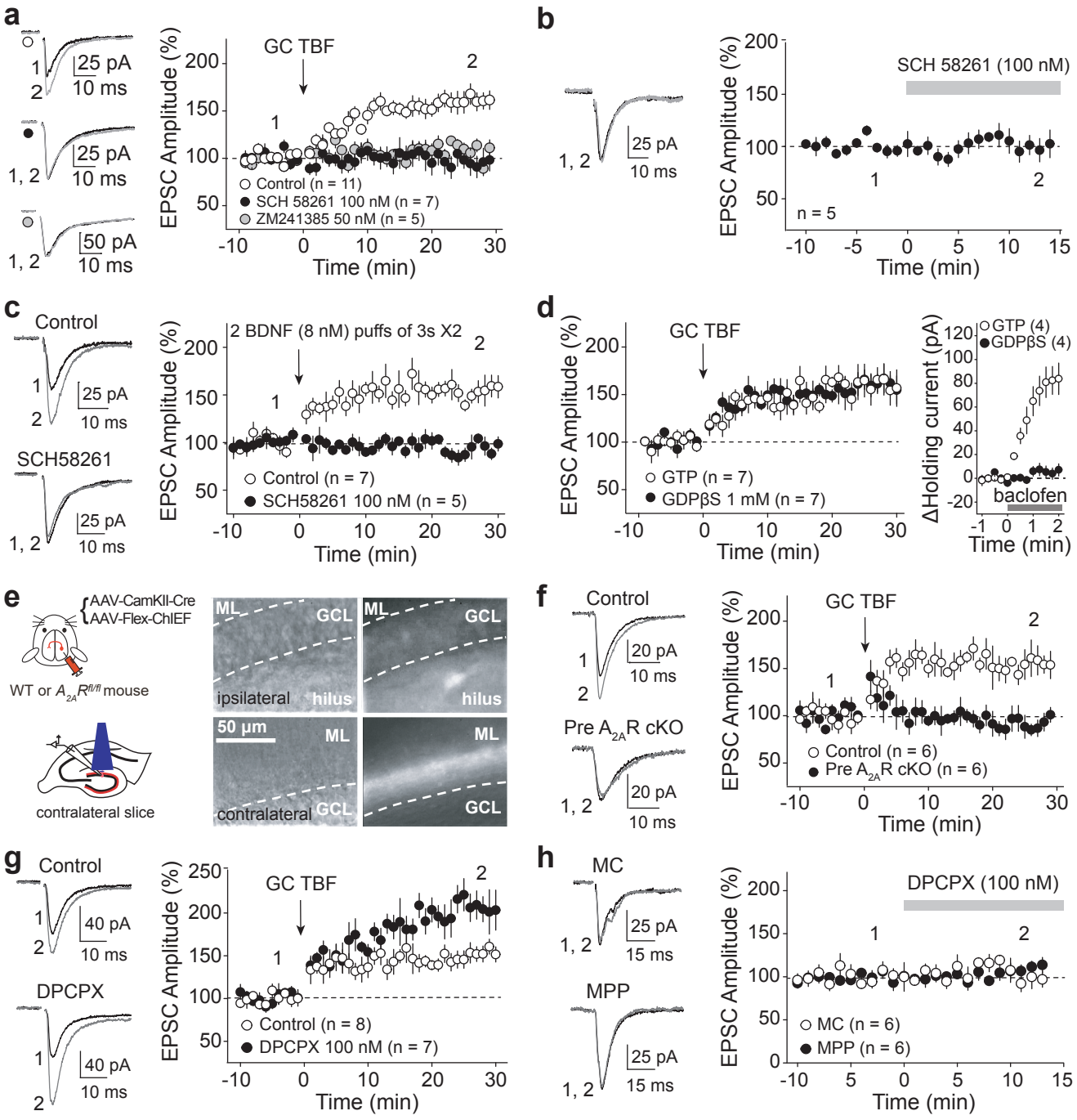
a
25 pA
10 ms
50 pA
10 ms
GC TBF
EPSC Amplitude (%)
Control (n = 11)
SCH 58261 100 nM (n = 7)
ZM241385 50 nM (n = 5)
Time (min)
b
25 pA
10 ms
SCH 58261 (100 nM)
n = 5
c
Control
SCH58261
2 BDNF (8 nM) puffs of 3s X2
Control (n = 7)
SCH58261 100 nM (n = 5)
d
GC TBF
GTP (n = 7)
GDPβS 1 mM (n = 7)
GTP (4)
GDPβS (4)
ΔHolding current (pA)
baclofen
e
AAV-CamKII-Cre
AAV-Flex-ChIEF
WT or A2AR fl/fl mouse
contralateral slice
ML
GCL
ipsilateral
hilus
50 µm
contralateral
f
Control
Pre A2AR cKO
20 pA
10 ms
Control (n = 6)
Pre A2AR cKO (n = 6)
g
Control
DPCPX
40 pA
10 ms
Control (n = 8)
DPCPX 100 nM (n = 7)
h
MC
MPP
25 pA
15 ms
DPCPX (100 nM)
MC (n = 6)
MPP (n = 6)

Figure 3

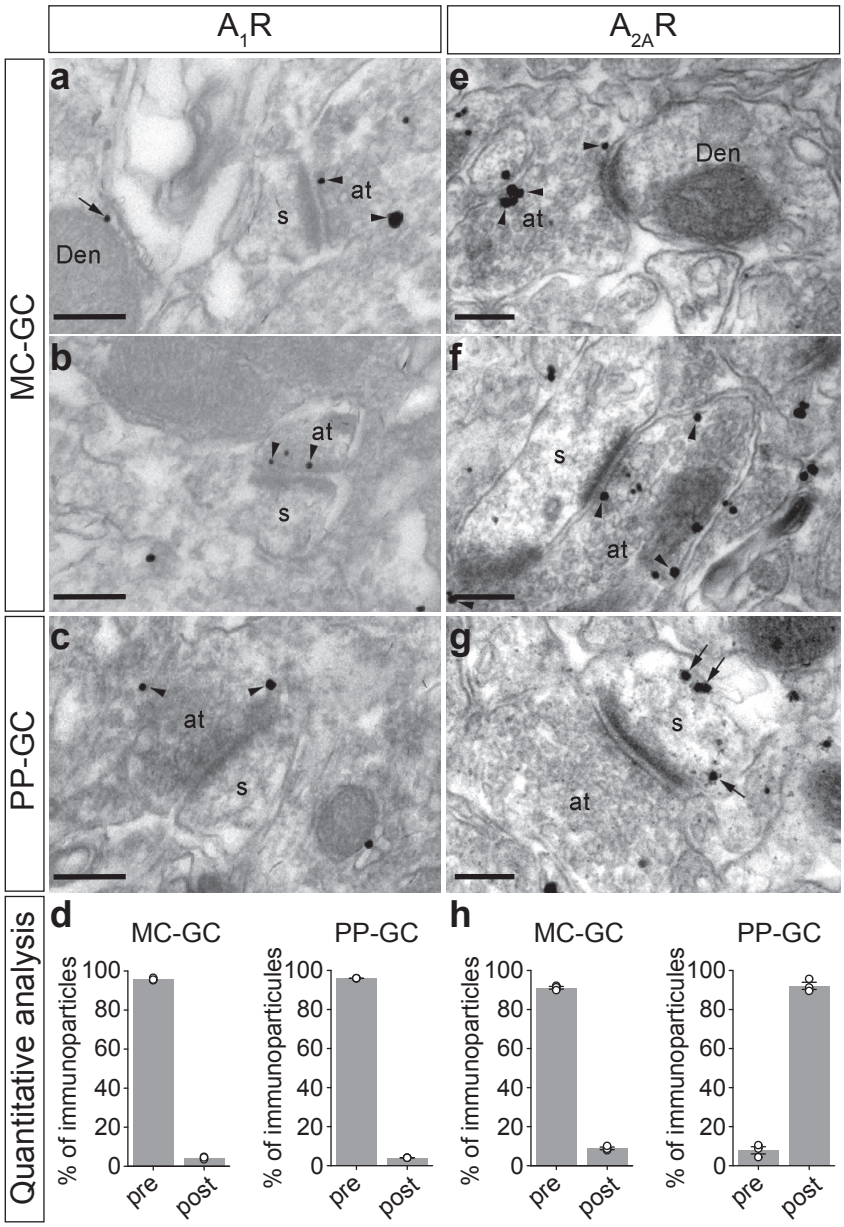
A1R
A2AR
MC-GC
PP-GC
Quantitative analysis
a
b
c
d
e
f
g
h
Den
at
s
MC-GC
PP-GC
% of immunoparticles
pre
post
0
20
40
60
80
100

Figure 4

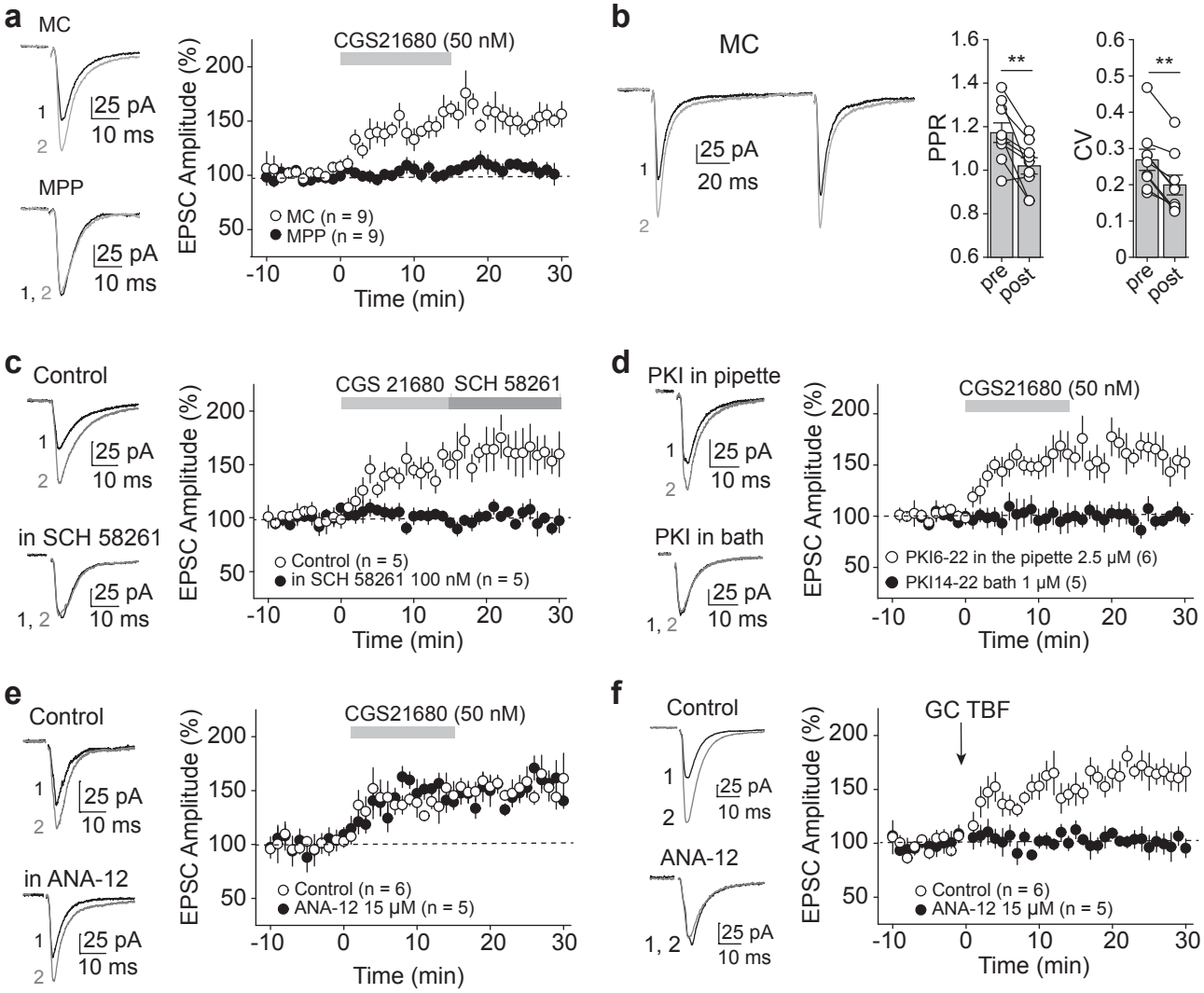
a
MC
1
2
25 pA
10 ms
MPP
1, 2
25 pA
10 ms
CGS21680 (50 nM)
EPSC Amplitude (%)
200
150
100
50
MC (n = 9)
MPP (n = 9)
-10
0
10
20
30
Time (min)
b
MC
25 pA
20 ms
PPR
CV
**
pre
post
c
Control
in SCH 58261
CGS 21680 SCH 58261
Control (n = 5)
in SCH 58261 100 nM (n = 5)
d
PKI in pipette
PKI in bath
CGS21680 (50 nM)
PKI6-22 in the pipette 2.5 µM (6)
PKI14-22 bath 1 µM (5)
e
Control
in ANA-12
CGS21680 (50 nM)
Control (n = 6)
ANA-12 15 µM (n = 5)
f
Control
ANA-12
GC TBF
Control (n = 6)
ANA-12 15 µM (n = 5)

Figure 5

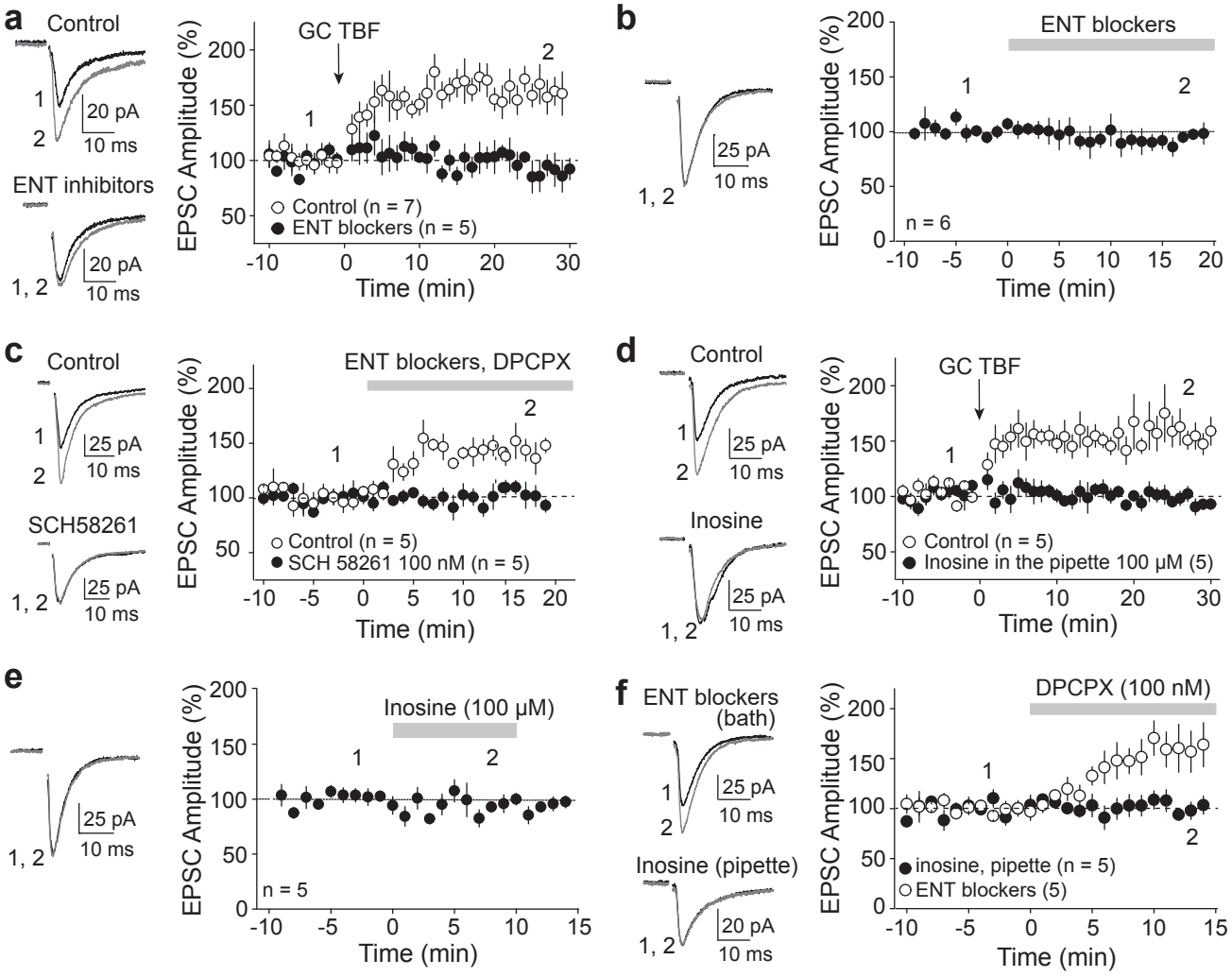
a
Control
1
2
20 pA
10 ms
ENT inhibitors
1, 2
20 pA
10 ms
GC TBF
EPSC Amplitude (%)
Control (n = 7)
ENT blockers (n = 5)
Time (min)
b
1, 2
25 pA
10 ms
ENT blockers
n = 6
Time (min)
c
Control
25 pA
10 ms
SCH58261
1, 2
25 pA
10 ms
ENT blockers, DPCPX
Control (n = 5)
SCH 58261 100 nM (n = 5)
Time (min)
d
Control
25 pA
10 ms
Inosine
1, 2
25 pA
10 ms
GC TBF
Control (n = 5)
Inosine in the pipette 100 μM (5)
Time (min)
e
1, 2
25 pA
10 ms
Inosine (100 μM)
n = 5
Time (min)
f
ENT blockers (bath)
1
2
25 pA
10 ms
Inosine (pipette)
1, 2
20 pA
10 ms
DPCPX (100 nM)
inosine, pipette (n = 5)
ENT blockers (5)
Time (min)

Figure 6

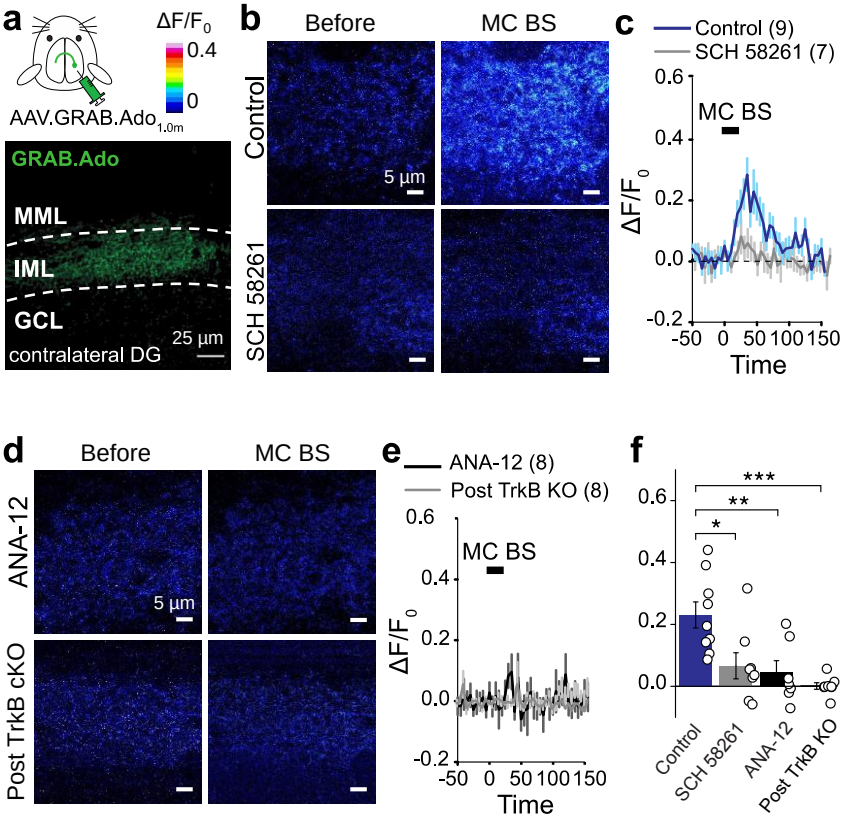

Figure 7

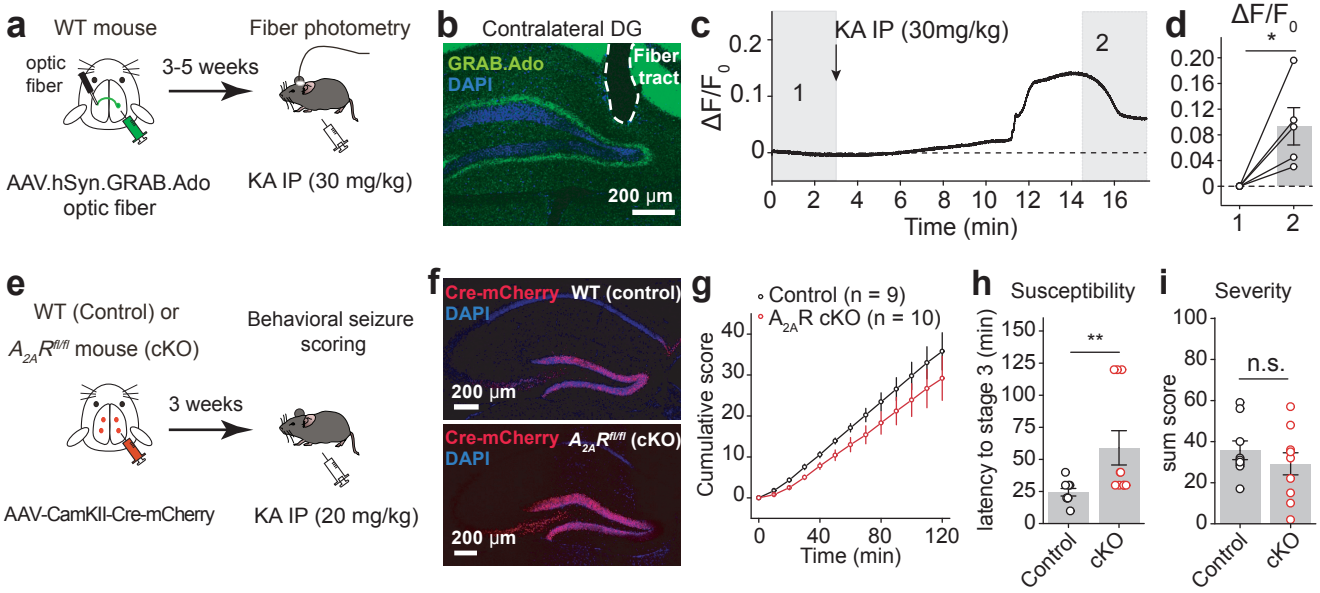
a
WT mouse
Fiber photometry
optic fiber
3-5 weeks
AAV.hSyn.GRAB.Ado optic fiber
KA IP (30 mg/kg)
b
Contralateral DG
GRAB.Ado
DAPI
Fiber tract
200 μm
c
KA IP (30mg/kg)
ΔF/F0
Time (min)
d
ΔF/F0
e
WT (Control) or
A2ARfl/fl mouse (cKO)
Behavioral seizure scoring
3 weeks
AAV-CamKII-Cre-mCherry
KA IP (20 mg/kg)
f
Cre-mCherry WT (control)
DAPI
200 μm
Cre-mCherry A2ARfl/fl (cKO)
DAPI
200 μm
g
Control (n = 9)
A2AR cKO (n = 10)
Cumulative score
Time (min)
h
Susceptibility
latency to stage 3 (min)
Control
cKO
i
Severity
sum score
n.s.
Control
cKO

Figure 8